February 2017
Doctor's Degree Thesis

Nanostructured Piezoelectric and Textile based Triboelectric Generator for Wearable Energy Harvesting System

Graduate School of Chosun University

Department of IT Fusion Technology

A Young Choi

Nanostructured Piezoelectric and Textile based Triboelectric Generator for Wearable Energy Harvesting System

웨어러블 에너지 하베스팅 시스템을 위한
나노구조 기반 압전 및 텍스타일 기반
마찰전기 제너레이터

February 24, 2017

Graduate School of Chosun University

Department of IT Fusion Technology

A Young Choi

Nanostructured Piezoelectric and Textile based Triboelectric Generator for Wearable Energy Harvesting System

Advisor: Prof. Youn Tae Kim

This thesis is submitted to The Graduate School of Chosun University in partial fulfillment of the requirements for the Doctor's degree.

October 2016

Graduate School of Chosun University

Department of IT Fusion Technology

A Young Choi

This is to certify that the Doctor's Thesis of A Young Choi

has been approved by the Examining Committee for the thesis requirement for the Doctor's degree in IT Fusion Technology.

Committee Chairperson
Prof. Sung Bum Pan _____ (Sign)

Committee Member
Dr. Myung-Ae Chung _____ (Sign)

Committee Member
Prof. Eun Seo Choi _____ (Sign)

Committee Member
Prof. Hyun-Sik Choi _____ (Sign)

Committee Member
Prof. Youn Tae Kim _____ (Sign)

December 2016

Graduate School of Chosun University

Table of Contents

List of Figures

List of Tables

Acronyms

PVDF	Polyvinylidene fluoride
PZT	Lead Zirconate Titanate
MEMS	Microelectromechanical System
LLO	Laser Lift-off
EAP	Electroactive Polymer
TENG	Triboelectric Nanogenerator
NFES	Near-field Electrospinning
FFES	Far-field Electrospinning
LED	Light Emitting Diode
SEM	Scanning Electron Microscope
CT-TEG	Corrugated Textile based Triboelectric Generator

요 약

웨어러블 에너지 하베스팅을 위한 나노구조 기반 압전 및 텍스타일 기반 마찰전기 제너레이터

최아영
지도교수: 김윤태 교수, Ph. D.
조선대학교 대학원 IT융합학과

웨어러블 에너지 하베스팅은 대규모의 발전 장치부터 소형 나노기기까지 다양한 분야에 응용하는 연구가 이루어지고 있다. 특히, 텍스타일형 마찰전기 에너지 하베스팅 기술은 인체 착용이 유용할 뿐만 아니라 유연하고, 가볍고, 편안하기 때문에 유망한 연구이다. 본 연구에서는 웨어러블 에너지 하베스팅을 위한 시스템을 구현하기 위해 압전 및 마찰전기 제너레이터를 개발하였다. 전기방사 공정을 이용하여 재료의 농도, 니들-컬렉터 거리 등의 조건에서 가장 균일하게 압전 나노파이버를 형성할 수 있는 공정 조건을 최적화하였다. 또한 스트레칭 동작에서 에너지 생산이 가능한 주름 구조의 텍스타일형 마찰전기 제너레이터를 제시한다. 본 연구에서 제안하는 텍스타일형 TEG는 텍스타일이라는 재료의 특성을 이용하여 박음질을 통해 주름구조를 제작하였으며 추가적인 지지대 없이 에어갭을 생성하였다. 결과적으로, 압력을 가하고 문지르는 행동뿐만 아니라 스트레칭 동작에서도 에너지 생성 가능한 것을 확인하였다. 약 140%에서 스트레칭/회복 동작을 반복하였을 때 30.3V의 결과 값을 보여주었다. 또한, 다양한 신체 활동에서 에너지가 생성되는 것을 확인하였다. 이 결과로 주름구조 텍스타일 기반 TEG는 자가 파워 시스템이 될 수 있는 잠재력을 보여주었다.

I. Introduction

1.1 Introduction for Energy Harvesting

1.1.1 Definition of Energy Harvesting

Energy harvesting is one of the most promising techniques for solving the energy problem without depleting natural resources. It is motivated by a desire to address the issues of climate change and global warming. General electronic devices operate using batteries. Unfortunately, these batteries must be replaced or recharged regularly. Energy harvesting can aid in replacing batteries and extending battery life. Energy harvesting is a technology that converts natural energy such as solar energy, wind energy, thermoelectric energy, or vibration energy to electrical energy. Recently, many studies have been focusing on self-powered energy sources that supply wearable and implantable devices with semi-permanent energy, thereby avoiding the need for external power sources.

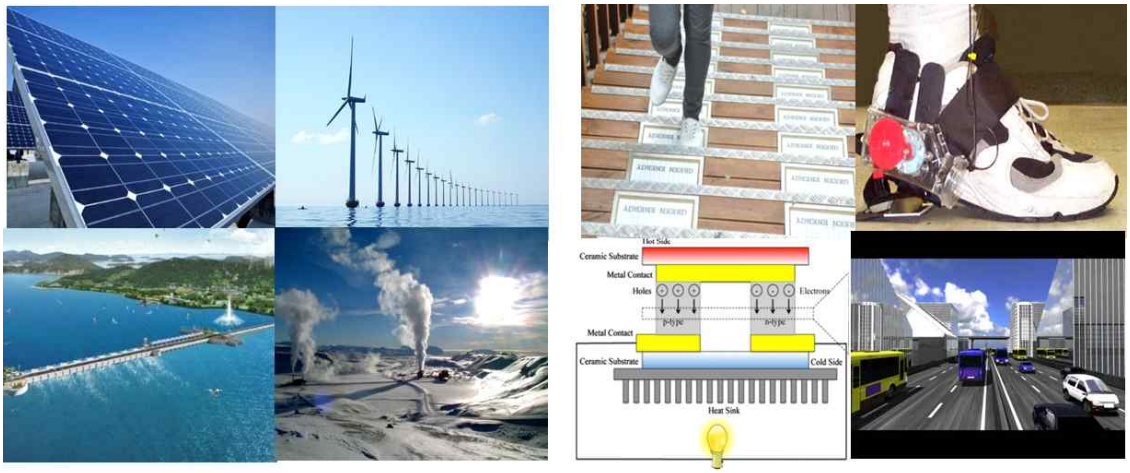

Figure 1.1. Energy sources for energy harvesting.

Human body/motion	Transportation	Infrastructure	Industry	Environment
Breathing, blood flow/pressure, exhalation, walking, arm motion, finger motion, jogging, talking	Aircraft, automobile, train, tires, tracks, peddles, brakes, turbine engine, vibration, noises	Bridges, roads, tunnels, farm, house structure, control-switch, water/gas pipes, AC system	Motors, compressor, chillers, pumps, fans, vibrations, cutting and dicing, noise	Wing, ocean current/ wave, acoustic wave

Table 1.1 Sources of mechanical energy around us that can be used for harvesting electricity [1].

1.1.2 Energy Sources

Energy harvesting is the process of capturing ambient energy and storing it in the form of electricity. The four main ambient energy sources present in our environment are solar energy, RF energy, thermal energy, and mechanical energy. A solar cell is a device that converts light energy into electrical energy. The form of energy exploited is light energy obtained usually from sunlight. However, solar energy is disadvantageous in terms of generating electricity, because it is often restricted by weather and location. A thermoelectric generator is a solid-state device that converts heat directly into electrical energy through a phenomenon called the Seebeck effect. However, it demonstrates a low energy conversion efficiency rate and requires a constant heat source.

Mechanical energy is one of the commonly available power sources for mobiles, portable electronics, and wireless sensing networks. Mechanical energy can be from a vibrating structure or a moving object. The mechanical-to-electrical energy conversion can be realized through basic mechanisms such as electromagnetic [2-4] and piezoelectric [5] effects. However, the voltage outputs of electromagnetic energy harvesting are typically very low and must be amplified to a sufficiently high level to charge

storage devices. Moreover, electromagnetic energy harvesters are difficult to fabricate in the microscale because of the poor properties of planar magnets and the limit to the numbers of turns using planar coils. Recently, piezoelectric generators using mechanical energy have been attracting considerable interest owing to their high output power generation. The piezoelectric harvesters output voltages that can be used directly. In addition, piezoelectric harvesters can be fabricated at microscales owing to the availability of well-established deposition techniques [6-7]. Furthermore, these can be fabricated as appealing wearable systems for use in wireless power sources, as human motion can generate mechanical power regardless of the surrounding environment.

A triboelectric generator is based on the electrification effect and electrostatic induction. In a triboelectric generator, energy is generated through the charge transfer that occurs during the physical contact between two materials that have different triboelectric polarities. Thus, wearable triboelectric generators driven by body motion have great potential in electric power supplies. This approach can be considered as a promising candidate for high-performance and stable nanogenerators that can be used in self-powered wearable electronics in the near future.

II. Wearable Energy System

2.1 Introduction to Wearable Energy System

Wearable energy system is a technology that can convert various forms of energy existing in the usual surroundings to electrical energy, and transmit to electrical devices. Recently, with the increase in the use of portable and wearable electric devices such as smartphones, smartwatches, and healthcare monitoring systems, the requirements on the power supplies in mobile environments have been increasing. In this situation, the energy originating

from human activity is drawing much attention. Wearable energy systems for humans can act as useful mobile powering systems because they can provide stable and sustainable power irrespective of the environmental conditions such as weather.

Textiles have been synonymous with human activity for thousands of years, and as the years have progressed, their usage has become wider and more varied. If a textile-based energy generator for a wearable energy system can be fabricated, a new energy generation and transmission framework can be created.

In this study, two studies on wearable energy harvesting technologies based on textiles are introduced. These are especially focused on the availability of the energy harvester.

2.2 Technologies for Wearable Energy Systems

2.1.1 Wearable Energy Harvesting

A wearable energy harvesting system utilizes the abundant mechanical energy generated by human bodies in everyday life. Human-activity-based energy harvesting, in the form of wearable devices, can easily harvest the energy generated from activities, and convert and store this energy in the form of electricity. The energy harvester is a relatively small power generator that does not require fossil fuels. It uses the energy available in the ambient environment, such as vibration, wind, water flow, and thermal energy. The harvested energy supplies operating power for portable and wearable IT devices. It is essential to assess the amount of energy that can be harvested from human activities, and to consider the different types of wearable devices, to effectively harvest electricity from mechanical energy. Wearable energy harvesting extracts energy from the human body itself. The potential sources

include body heat and motion. Two types of energy sources can be used for harvesting in wearable devices. These are the mechanical energy from people's movements or acceleration during transport, and the heat flow caused by the difference in temperature between the human body and the ambient environment.

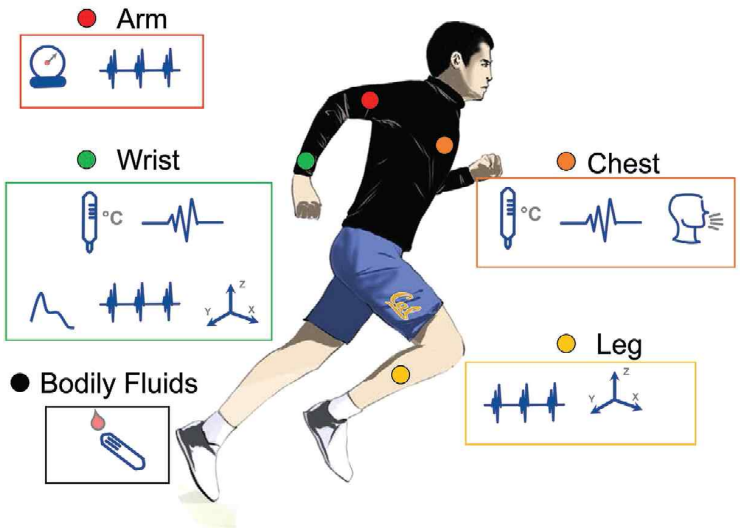

Figure 2.1. Location of energy harvesting module[8].

The figure 2.2 shows the flexible Bi_2Te_3/Sb_2Te_3 thermoelectric generator developed on a on a glass fabric[9]. The voltage of a thermoelectric generator is proportional to the temperature difference. However, the difference between body temperature and air temperature is relatively small, giving millivolt-level voltages for a single generator.[9-12] Wearable thermoelectric generators have been used to power a number of devices such as glucose sensor[13], electroencephalogram[14] and pulse oximeter[15].

Figure 2.2. Flexible thermoelectric generator.

The various movements of the human body, including walking, moving limbs, flexing muscles, and breathing are the sources of energy that can be used to generate power. The energy available in these motions, which varies over several orders of magnitude as indicated in Table 2.1, can be harvested using wearable piezoelectric or triboelectric generators. Flexible piezoelectric generators have recently been developed based on more flexible forms of lead zirconate titanate (PZT), such as thin ribbons [16] or nanowires [17], as well as those of lead-free materials such as ZnO nanowires or polyvinylidene fluoride (PVDF) [18-22]. Triboelectric generators generate electricity from the transfer of surface charges, which occurs when certain materials including metals and polymers are brought into contact. Piezoelectric and triboelectric sensors have been used to harvest energy from the motion of joints such as wrists, fingers, elbows, and knees [18-19].

Figure 2.3 shows a piezoelectric generator developed by Siddiqui et al. for use on the finger, wrist, or elbow, and the corresponding voltages as each of those joints are bent [19]. Figure 2.4 shows the voltage from a triboelectric generator developed by Yang et al. for use at the elbow and bicep [23]. Wearable piezoelectric and triboelectric generators can be integrated into

textiles to harvest energy from human motion.

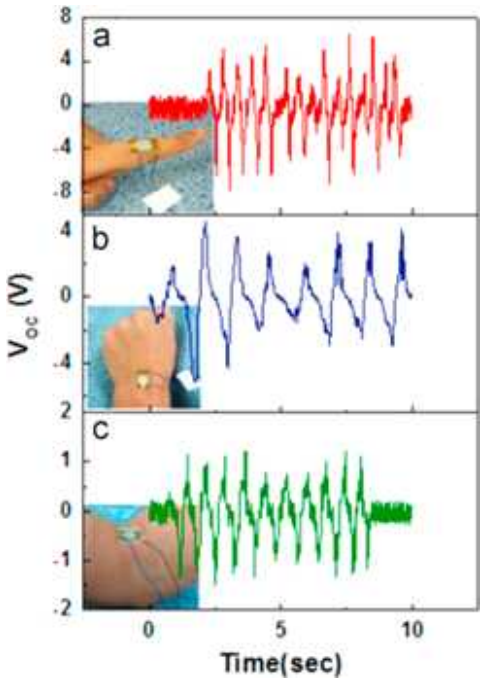

Figure 2.3. Output voltage when attached to finger, wrist and elbow.

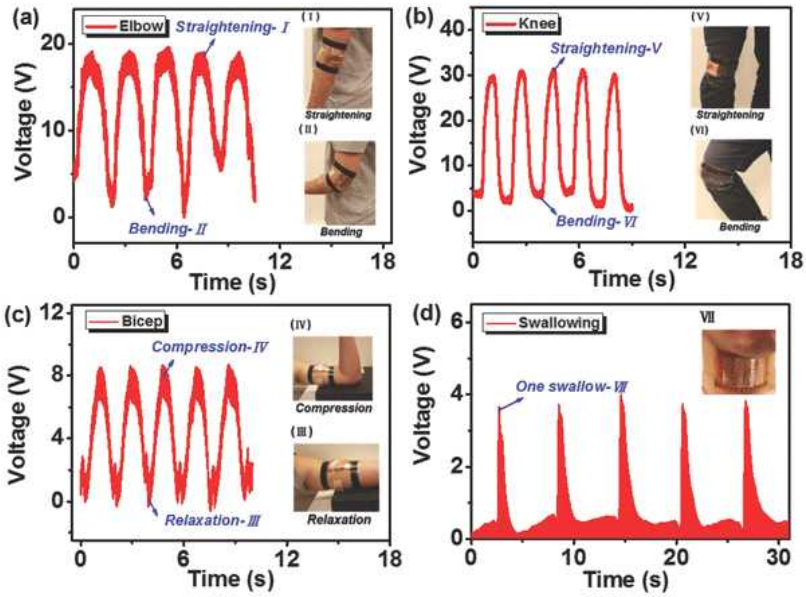

Figure 2.4. Output voltage triboelectric generator.

Source	Collection mechanism	Power density	Advantages
Body heat	Thermoelectrics	10 s of μW cm^{-2}, DC	Reliable, potential for self-powered temperature sensing
Body motion	Piezoelectrics, triboelectrics	<1 to 100 s of μW cm^{-2}, depending on type of motion, AC	High power for some motions, potential for self-powered heart rate and respiration sensing

Table 2.1. Characteristics of energy sources for wearable devices[24].

Consequently, the wearable energy harvesting system provides the best solution for individuals who are in need of an immediate and reliable power supply. Wearable energy harvesting systems will help in greatly improving the convenience in people's lives and in expanding the applications of personal electronics.

2.2.2 Technology of Wireless Power Transmission

Wireless energy transmission is the transmission of electrical energy from a power source to an electrical load. The transmission of power through air has been around for a century, with Nikola Tesla's pioneering ideas and experiments being perhaps the most well-known early attempt to do so. The power transmission technology is currently being used to charge portable devices wirelessly [25]. In addition, an international standard has been developed for wireless body area networks that enable communication among various sensors that monitor human physical conditions [26]. Figure 2.5 shows the methods of wireless power transmission such as electromagnetic induction, magnetic resonance, and radiowave technology. Capacitive coupling is a method of transmitting power through the capacitive coupling between opposing plane electrodes. Electromagnetic induction is the transmission of power using the current induced by the magnetic field between opposing coils. Magnetic resonance transmits power over space, utilizing the resonance phenomenon based on the same principle as electromagnetic induction. Radiowave technology generates power from the radiowaves received by an antenna.

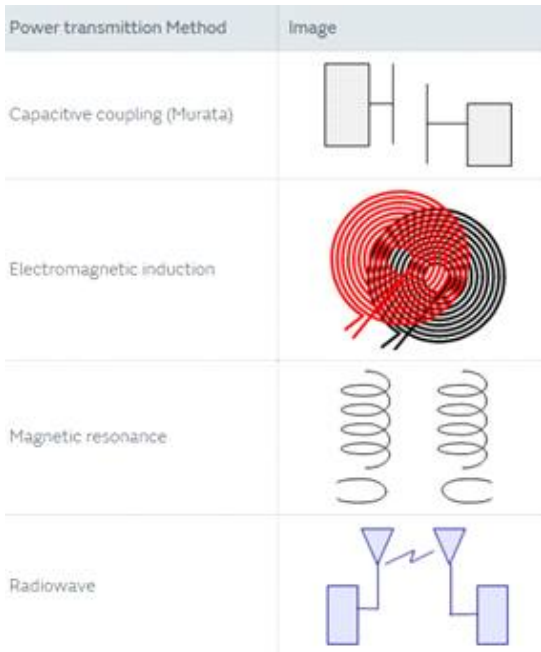

Figure 2.5 Methods of power transmission.

Figure 2.6 shows the wireless power transmission technology based on magnetic resonant coupling, which uses resonant coils made of conductive yarn instead of copper wire. Thus, they can be easily integrated into clothing [27].

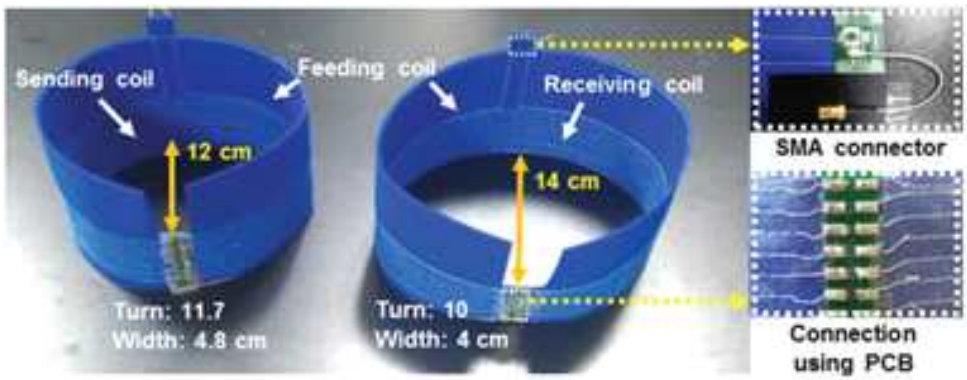

Figure 2.6 Resonant coils made of conductive yarn embroidered on nonwoven polyester fabric.

III. Nanostructured Piezoelectric Generator

3.1 Introduction

Ubiquitous energy sources and energy harvesting technologies capable of charging energy at any place and at any time have become popular research topics. Portable and mobile devices such as smart phones, tablet PCs, and smart watches have been developed in the last several decades. The battery technologies have been improved to help people use these devices for an extended period. However, these devices still suffer from limited usage time due to the additional power consumption from the added operations and components. Consequently, continuity of power supply is the most essential condition for mobile devices.

Many energy harvesting technologies have been proposed to convert the energy that can be obtained from usual surroundings into electricity. Many researchers have attempted to supply power to mobile devices in real-time using the energy generated from the human body. These studies include knee-mounted generators, harvesting energy from breathing, and textile-type energy generators. Human motion can be used effectively by designing structures that can be mounted on unique locations on the human body or that are wearable.

The electrospun nanofiber piezoelectric generator fabricated far-field electrospinning (FFES). Electrospinning is an efficient technique for the fabrication of nanoscale fibers. In this technique, a solution is extruded through nanoscale spinnerets, and the spun fibers are collected on a grounded plate.

This piezoelectric generator study proposes that the piezoelectric outputs of the electrospun nanofibers fabricated by FFES can be improved by an additional poling process. Highly enhanced piezoelectric and flexible

nanocomposite electrospun fibers were fabricated through the FFES processing of a solution contaning barium titanate($BaTiO_3$) and styrene-ethylene-butylene-styrene (SEBS).

3.2 Theoretical Background of Piezoelectric Generator

3.2.1 Definition of Piezoelectricity

Piezoelectric effect is the ability of certain materials to generate an electric charge in response to applied mechanical stress. One of the unique characteristics of the piezoelectric effect is that it is reversible, meaning that materials exhibiting the direct piezoelectric effect (generation of electricity when stress is applied) also exhibit the converse piezoelectric effect (generation of stress when an electric field is applied). Intrinsic factors include the frequency constant of the piezoelectric element, piezoelectric and mechanical properties of the materials, and temperature and stress dependence of the physical properties.

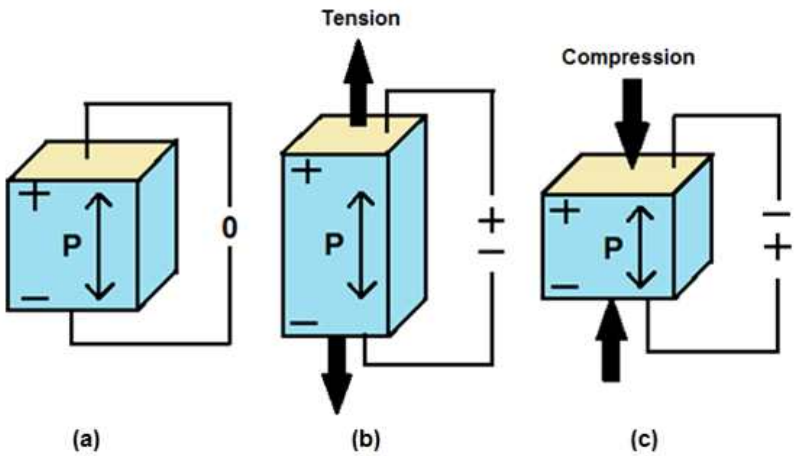

Figure 3.1. Piezoelectric effect.

An electric field generates various stresses and deformations according to the direction of the electric field applied in the direction of dipoles. For example, d_{33} is a piezoelectric charge constant when deformation occurs in the direction of the electric field applied in one directional and d_{31} is a piezoelectric charge constant where if an electric field is applied in the "3" direction, deformation occurs in the "1" direction.

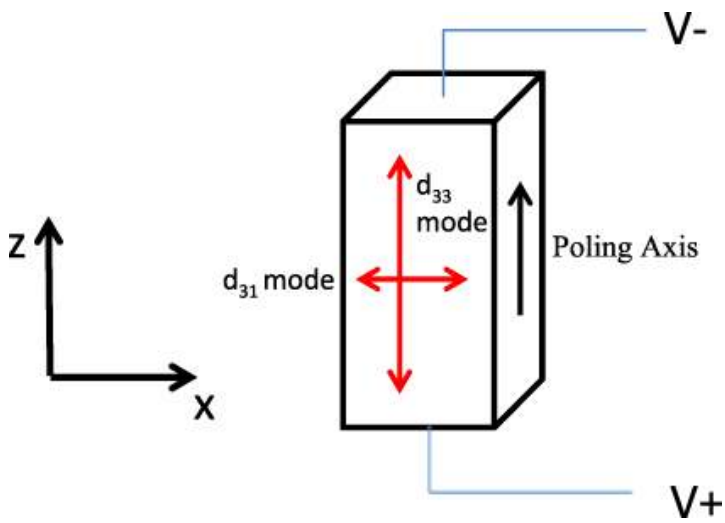

Figure 3.2. Coupling mode of piezoelectric generator.

3.2.2 Piezoelectric Material

Piezoelectric materials create electric charges in response to the polarization induced by mechanical stress. They involve the interconversion of mechanical and electric energies, as discovered by Curie in 1880.

Piezoelectric materials include $BaTiO_3$, PZT and PVDF. These materials are ferroelectrics having molecular structures with polarizations in the same direction and having electric dipole characteristics. Commonly, a random electric dipole is rearranged along the electric field if heated above the Curie

temperature when a strong electric field is applied. This process is called poling.

3.2.3 Piezoelectric Poling

Through this poling (Figure 3.3) treatment, domains that are nearly aligned with the electric field expand at the expense of domains that are not aligned with the field, and the element lengthens in the direction of the field. When the electric field is removed, most of the dipoles are locked into a configuration of near alignment. The element now has a permanent polarization —the remnant polarization—and is permanently elongated.

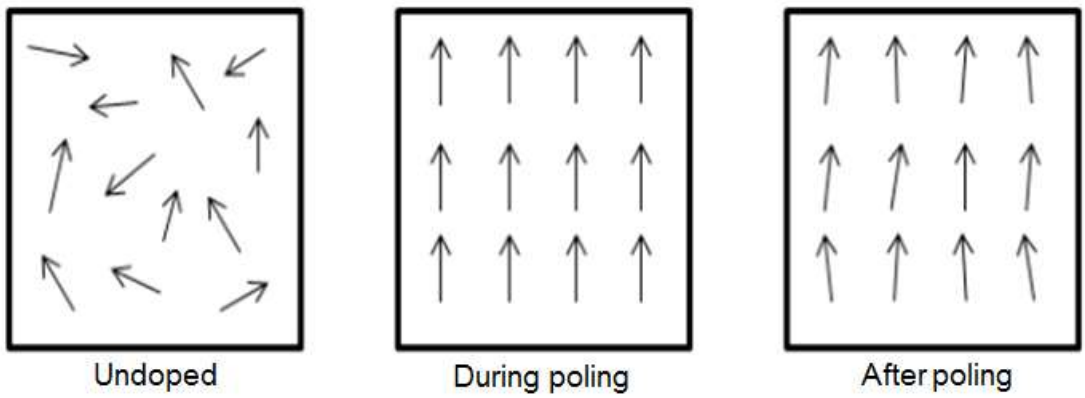

Figure 3.3. Polling process (a) random orientation of polar domains prior to polarization (b) polarization in DC electric field (c) remanent polarization after electric field removed

3.2.4 Background of Piezoelectric Generator

Piezoelectric generators have been used for many years to convert mechanical energy into electrical energy. Numerous studies have been reported since a Georgia Tech research team first reported a nanogenerator using ZnO

nanowires in 2006 [28].

a. Piezoelectric Cantilevers

The cantilever-type piezoelectric harvester is one of the most widely used architectures because it can produce larger mechanical strains in the piezoelectric material under vibration conditions. Additionally, its fabrication is simple and inexpensive. A general structure of the cantilever-type piezoelectric energy harvester is illustrated in Figure 3.4.

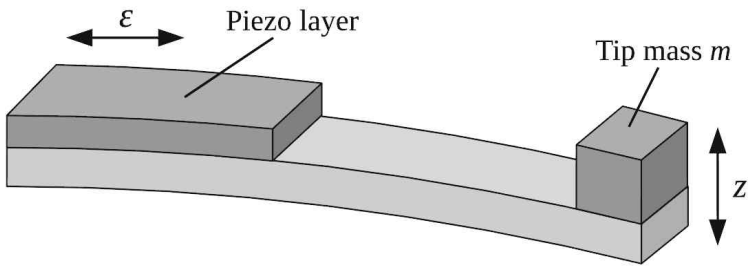

Figure 3.4. Cantilever type piezoelectric energy harvester.

b. MEMS Piezoelectric Energy Harvesters

The microelectromechanical system (MEMS) technology is one of the promising technologies that utilize the low flexural rigidity of the piezoelectric energy harvesting devices. Figure 3.5 shows a $BaTiO_3$-film-based flexible nanogenerator. It consists of metoal-insulator $BaTiO_3$-metal structure ribbons. Poled ferroelectric $BaTiO_3$ thin films were transferred to a plastic substrate through conventional microfabrication and soft lithographic techniques. The $BaTiO_3$ nanogenerator converted mechanical energy (bending motion) into electrical energy.[29]

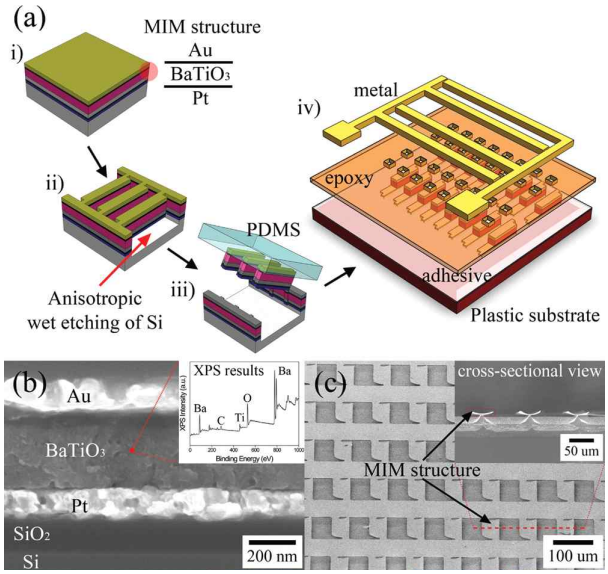

Figure 3.5. Schematic illustration of flexible $BaTiO_3$ nanogenerator.

Figure 3.6 shows soft and flexible PZT textiles with nanowires parallel to each other. PZT nanowire arrays are epitaxially grown on conductive substrates using a hydrophermal method. The PZT nanowire textile nanogerator has a high piezoelectric coefficient ceramic nanowire, and is a soft, flexible, and wearable piezoelectric generator, which is valuable for portable devices [30].

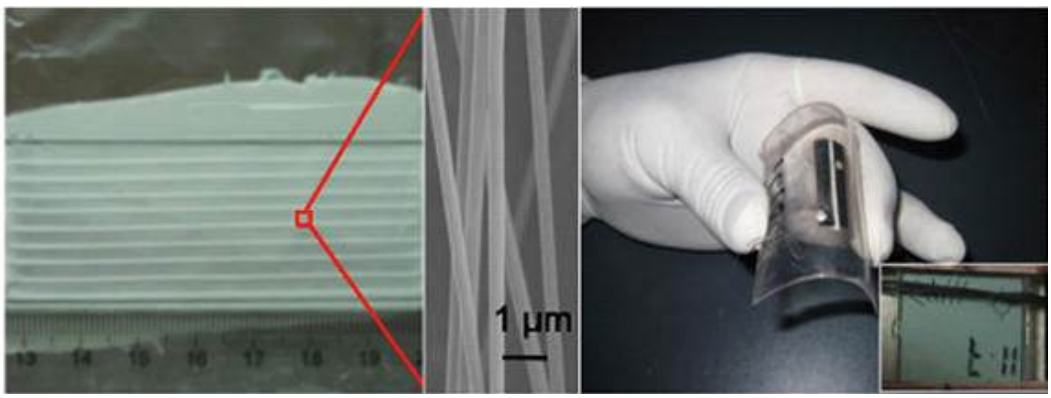

Figure 3.6. PZT nanowire textile nanogenerator.

Figure 3.7 shows a PVDF-PZT nanocomposite film. The PVDF-PZT nanocomposite film demonstrates self-charging a Li battery using a PVDF-PZT nanoparticle composite separator, leading to good energy conversion/storage efficiency. PZT nanoparticles intensify the piezoelectric potential, because of the geometrical strain confinement effect. More pores in composite files result in high piezo potential and more ionic conduction paths [31].

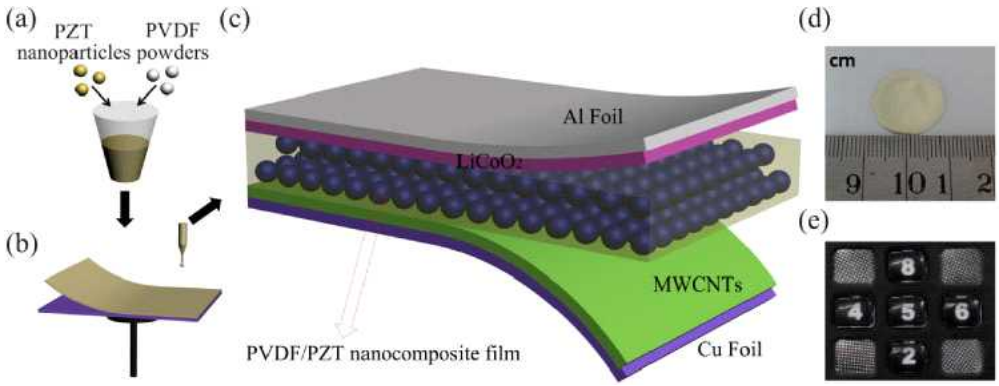

Figure 3.7. PVDF-PZT nanocomposite film.

Thin-film materials also have remarkable potential for piezoelectric energy harvesting. Figure 3.8 illustrates a transparent flexible piezoelectric energy harvester based on the laser lift-off (LLO) process. These transparent devices based on PZT films generate power during the periodical bending and releasing motion [32].

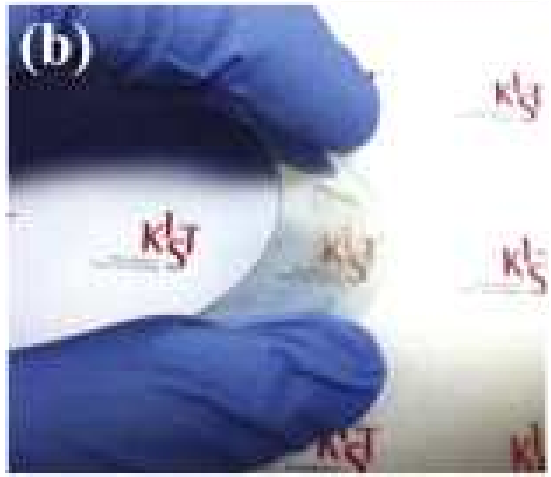

Figure 3.8. Transparent flexible devices based on PZT film.

c. Applications of Piezoelectric Energy Harvesters

Innowattech in Israel developed a piezoelectric energy generator using piezoelectric polymers [33]. This company proposed a self-generating technology to supply power in a smart manner, and installed it at railroads and roads. An MIT team, funded by the Defense Advanced Research Project Agency (DARPA), fabricated a generator prototype that could produce 0.9 to 3 mW when a dielectric elastomer electroactive polymer (EAP) was applied in military boots [34].

Figure 3.9. Example of piezoelectric energy harvester.(Innowattech)

3.3 Materials

3.3.1 Polyvinylidene difluoride (PVDF)

Polyvinylidene difluoride (PVDF) is a semicrystalline thermoplastic polymer with good mechanical and electrical properties, and attracts much interest because of its potential applications as a piezoelectric, pyroelectric, and ferroelectric material. Its piezoelectric coefficient is ~20 pC/N, which is higher than that of ZnO. The flexible polymeric nature allows very high strains to be applied to a PVDF beam, and thus, a high piezoelectric potential can be expected. PVDF is able to crystallize in five different forms, which involve three different chain conformations, namely, TTTT for β phase, TGTG' for α and δ phases, and TTTGTTTG' for ɣ and ε phases. Although each PVDF polymer chain has an effective molecular dipole moment, only the β and ɣ phases have dipole moments in the crystalline state. There are several methods to obtain the polar β phase of this polymer. These include mechanical stretching, poling, casting from solutions, spin coating, electrospinning, and use of additives like nanoclay. Moreover, poly(vinylidene fluoride–co–trifluoroethylene) (PVDF–TrFE) is attractive in industrial applications because of its high piezoelectricity among piezoelectric polymers, flexibility, low weight, and chemical stability.

3.3.2 Graphene

Graphene is a two-dimensional carbon material that is one atom thick; it is light and has extremely high strength, thermal stability, and electrical conductivity. Thus, graphene nanosheets are ideal “bricks” for fabricating nanocomposite structures with multifunctionality. A series of works has already been conducted on the use of nanosheets of graphene oxide or reduced graphene oxides as nanofillers to improve the electrical and thermal

conductivities or the strengths of polymers. However, the effects of the addition of reduced graphene oxide on the β phase formation have not been reported despite its superior electrical and mechanical properties.

3.4 Method

3.4.1 Principle of Electrospinning

Electrospinning is an attractive method for fabricating piezoelectric polymers because it enables fabrication of piezoelectric micro and nanofibers with high energy conversion efficiencies in one step. The electrospun nanofibers have attracted considerable attention because of their outstanding characteristics such as high porosity, small diameter, excellent pore interconnectivity, and high surface to volume ratio.

Electrospinning process involves the uniaxial stretching of a viscous polymer solution or melt in an electric field due to the electrostatic repulsions between the surface charges along the jet. Electrospinning of PVDF promotes the *TTTT* conformation and induces the formation of the β phase, possibly due to the highly extensional flow of the polymer solution [35]. This method also generates simultaneous poling of the solution to form a one-dimensional nanofiber from a viscous polymer solution.

This technique did not receive attention until the 1990s. However, after it was found that organic polymer nanofibers could be produced using electrospinning, it has been popularized, and the attention and research on electrospinning has increased significantly.

A typical electrospinning setup consists of a syringe, a collector, and a high-voltage power supply. The schematic of an electrospinning set up is shown in Figure 3.10. A syringe is filled with a melt and a polymer solution,

and a high voltage is applied between the syringe needle and the collector.

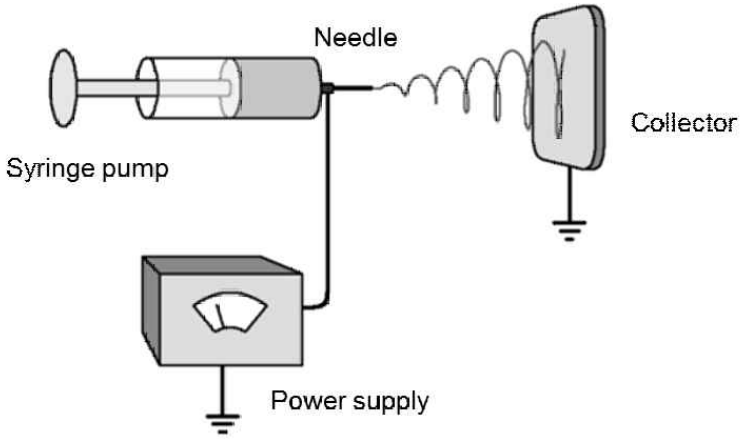

Figure 3.10. Schematic of electrospinning setup.

As the charged jet accelerates towards the region of lower potential, the solvent evaporates. The result of this electrostatic repulsion of the charged polymer causes the fibers to elongate.

Electrospinning results in a wide range of nanofibers made of polymers, polymer blends, or metal. They have been provided with different fiber morphologies such as aligned fibers, beaded, ribbon, porous, and core-shell.

Recently, the synthesis and design of nanosized inorganic and organic materials via electrospinning process have generated interest in the field of material sciences owing to their improved and enhanced properties and applicability. It is a simple and comfortable technique for the production of electrospun nanofibers. These electrospun nanofibers are used in the fields of energy, sensors, smart materials, regenerative medicine, and biotechnology. These nanocomposites contribute to producing light batteries [36-37], lightweight sensors [38], and fuel cells [39-42]. Electrospinning is less expensive and simpler than the conventional spinning process.

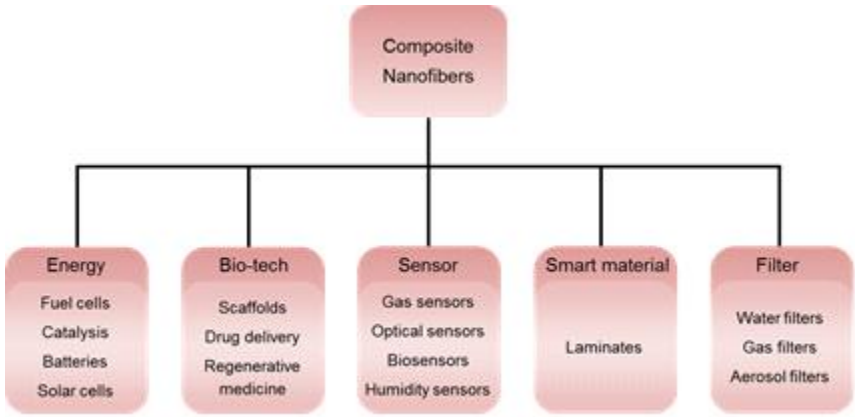

Figure 3.11. Applications of electrospun nanofibers.

3.4.2 Parameters of Electrospinning

Electrospinning involves many parameters. The solution parameters are viscosity, conductivity, molecular weight, and surface tension. The applied electric field, tip-to-collector distance, and flow rate constitute the process parameters. In addition, humidity and temperature play significant roles in determining the morphology and diameters of the electrospun nanofibers.

3.5 Experiment

3.5.1 Materials and solution preparation

A 15 wt% (w/w) polymer electrospinning solution was prepared by dissolving PVDF-TrFE (70:30 mol %, Piezotech, France) in acetone/DMAc (3:7; Sigma-Aldrich, USA).

3.5.2. Electrospinning process

Electrospinning of PVDF-TrFE was performed, and the characteristics of the electrospun nanofibers dependent on thickness were analyzed. The electrospinning setup consisted of a plastic syringe (5 ml) and a steel needle (i.d = 0.5 mm). The needle was connected to a high-voltage power supply (Nano Technics, Korea). The electrospun fibers were deposited on a 4 ´ 4 cm electrode collector. The solvent for the 15 wt% PVDF-TrFE was dissolving acetone/DMAc (3:7; Sigma-Aldrich, USA). Figure 3.12 shows the SEM images of 10, 15, and 20 wt% PVDF-TrFE. The diameter of the 10 wt% PVDF-TrFE is small, between 282 nm and 413 nm, but there is a lot of bead. The diameter of the 20 wt% PVDF-TrFE is nonuniformly distributed between 799 nm and 1.16 μm. On the other hand, the diameter of the 20 wt% PVDF-TrFE is between 590 nm and 719 nm. There is no bead and it presents an optimum condition than the 10 wt% and 20 wt% PVDF-TrFEs. The distance between the needle tip and electrode was 15 cm. The DC voltage applied by a high-voltage power supply (Nano Technics, Korea) was 15 kV.

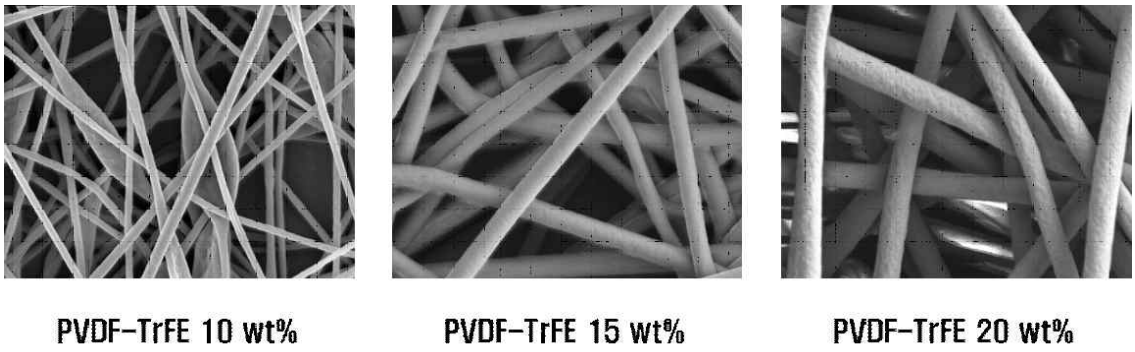

Figure 3.12. SEM images of PVDF-TrFE.

3.5.3. Preparation of PVDF-TrFE Electrospun fibers

To compare the performances of the top and bottom electrospun fibers, the fibers were separated by placing a sheet of paper (20-mm thick) over the as-prepared bottom electrospun fibers (» 30 mm), and performing electrospinning again on the paper to make the top electrospun fibers (» 30 mm) under the same conditions used previously. The casting film (» 30 mm) was prepared by spreading PVDF-TrFE electrospinning solution on the glass and drying for two days.

3.5.4. Preparation of $BaTiO_3$/SEBS electrospun fibers

The BaTiO3 for fabricating the electrospun fibers was dissolved in ethanol. The ethanol vaporized after the solution was stirred for 24 h at room temperature. SEBS was dissolved in chloroform and stirred for 24 h at room temperature.

3.5.5 Characterization

X-ray diffraction (XRD, DX-2500, China) was performed using Cu-$K_a$radiation(wavelength0.154nm)at40kVand30mA,toanalyzethecrystalstructureofPVDF-TrFE.

3.5.6 Electrical measurement

The electrospun nanofibers were forced using a pushing machine controlled by a force sensor, and the open circuit voltage of the mat inside the 2′-2-cm copper electrodes was measured using an oscilloscope (Tektronix, USA).

3.6 Results

In this study, the mechanism of additional poling process of electrospun nanofibers by local electric field which is originating from residual charges in far-field electrospinning process. The local electric field strength calculated by simulation was higher than reported electric field strength of near-field electrospinning (10 MV/m). Piezoelectric output measurement of poly(vinylidene fluoride-co-trifluoroethylene) electrospun nanofibers was performed by push test and output signals of bottom and top were compared, showing agreement with the trend of the simulation. It can be concluded that the piezoelectric outputs of electrospun nanofibers tend to be improved by residual charge.

Poly(vinylidene fluoride-co-trifluoroethylene) (PVDF-TrFE) is attractive in industrial applications because of their high piezoelectricity among piezoelectric polymers, flexibility, light weight and chemical stability [43]. However, stretching and poling processes are required for PVDF-TrFE to have piezoelectricity. Polar β-phase structure is induced by the stretching from non polar α-phase structure and molecular dipole is aligned by applied electric field called the poling process [44,45].

Electrospinning process provide the possibility of in situ mechanical stretching and electric poling to produce electroactive β-phase PVDF-TrFE electrospun nanofibers form its polymer solution. Electrospinning is an attractive method for fabricating piezoelectric polymer because it enables fabrication of piezoelectric micro- and nanofibers with high energy conversion efficiency in one step [46-48]. Near-field electrospinning (NFES) has been used to fabricate piezoelectric nanofibers because it provides an external electric field that is high enough (higher than 10 MV/m) to align the dipole [49]. Recently, piezoelectric bulky electrospun nanofibers have been fabricated by a conventional electrospinning method called far-field electrospinning (FFES) [50-54]. However, it is notable that piezoelectric output

of electrospun nanofibers can be achieved by week electric field (0.065 MV/m) in FFES [50], which is too small to align molecular dipole moment (only 0.65 % compared to that of NFES).

This propose that piezoelectric outputs of electrospun nanofibers fabricated by FFES can be improved by an additional poling process. A local electric field exerted by residual charges in electrospun nanofibers can play pivotal role in process of the additional poling. To investigate local electric field effect, we calculated the electric field strength by residual charge using simulation and the piezoelectric outputs of electrospun nanofiber mats were measured to compare the experimental result with simulation data.

The piezoelectric polymer is acquired by electrospinning in one step without additional process illustrated in Figure 3.13. When a electric field is applied to a needle tip containing polymer solution, the polymer solution is stretched by electric static force and the internal structure transform to the polar β-phase structure.[55,56] Also, molecular dipole in a electric field is forced to rotate to the field direction and consequently, molecular dipoles are oriented in one direction by the applied electric field.

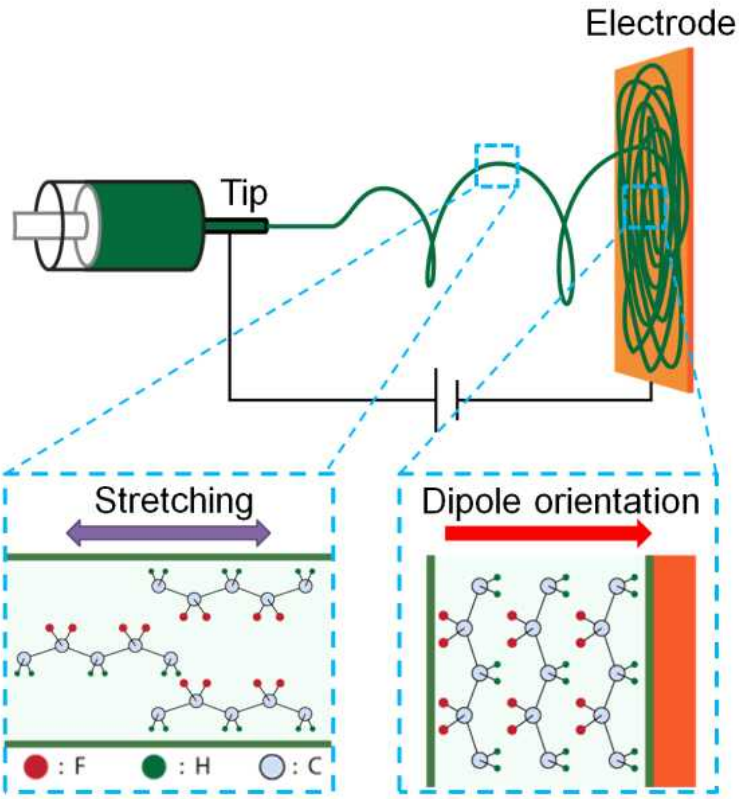

Figure 3.13. Schemes of the far-field electrospinning process.

In case of NFES, this electric field strength is enough to orient molecular dipole, however, the strength of FFES is only 0.7% ~ 2% of that of NFES. Because piezoelectric response increases as increasing electric field in poling process, electrospun nanofibers fabricated by the week field in FFES are expected to have weak piezoelectric output. However, the electrospun nanofibers show high piezoelectric output that were sufficient to light up a light emitting diode (LED).[53] For explaining the mechanism of dipole alignment by such a weak electric field, this suggest that not only applied electric field but also local electric field generated by residual charge can significantly contribute to alignment of molecular dipole, implying that piezoelectric response can be controlled by residual charge density.(Figure.

3.14)

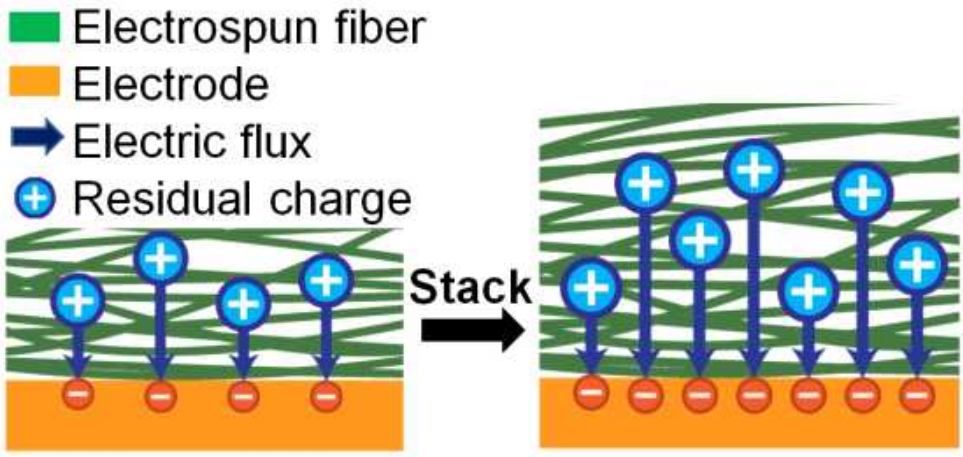

Figure 3.14. The local electric field is generated by residual charge.

Residual charges are the charges which are trapped in the solidified polymer after electrospinning process. Some polymers which are dielectric materials exhibit the ability to retain electric charges over long time, residual charges are remain after electrospinning. It is discovered in the experiment that the residual potential value generated by accumulating residual charge is enormous around 1kV and polymer fibers contained residual charge nearly adhere to electrode.[57] Therefore, the residual charges generate the local electric field between electrospun nanofibers and electrode, and the field strength is enough to align molecular dipole.[58-60] The electric field strength near the electrode increases as thickness increases.

To confirm that local electric field strength by residual charges is enough to align molecular dipole moment, it calculated the local electric field strength by residual charge using the simulation (COMSOL multiphysics 3.5a). This set up simulation conditions in which the gap between the electrode and the point substituted needle tip was 15 cm, an electrode of 4 x 4 cm was connected with the ground, the applied voltage was 15 kV, the stacked electrospun mat

thickness was 100 mm. This decide the residual charge density based on polymeric electrospun nanofibers[61-63] and charge densities per volume in simulation are assumed as 10, 20 and 30 C/m^3. When dissipation effect of residual charges during electrospinning is ignored, the electrospun mat containing the residual charge can be assumed as charged thin insulating layer. According to Gauss's law, the electric field strength is dependent on the total charges on the Gaussian surface. In particular for film, the electric field from E can be written as[59]:

$$\frac{\sigma}{\epsilon'\epsilon} = \frac{\sigma' t}{\epsilon'\epsilon} \qquad (1)$$

where σ is the surface charge density, σ' is the charge density per volume of fibers, t is thickness of electrospun mat, ϵ' is the relative permittivity of PVDF-TrFE and ϵ is the permittivity of vacuum. From Eq. (1), the electric field strength increases as the charge density per volume and thickness of the electrospun mat increase. Charge density per volume value is affected by electrospinning conditions such as material, solvent, concentration of solution and applied voltage. Eq. (1) implies that the local electric field strength can be controlled by the electrospinning condition.

The SEM image figure 3.15 shows the electrospun fibers. PVDF-TrFE fibers deposited on the electrode randomly distributed without beads.

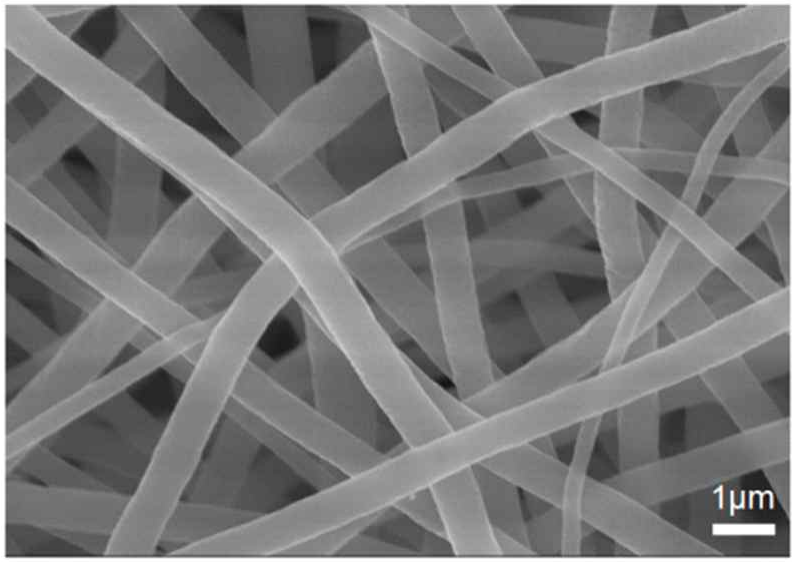

Figure 3.15. SEM image of randomly electrospun PVDF-TrFE fibers

Figure 3.16 presents the diameter distribution of 100 counted PVDF-TrFE fibers using the SEM image. The average diameter of electrospun fibers is ~800 nm in the range from ~300 to ~1300 nm and the diameter of fibers is between 600 and 900 nm above 75%.

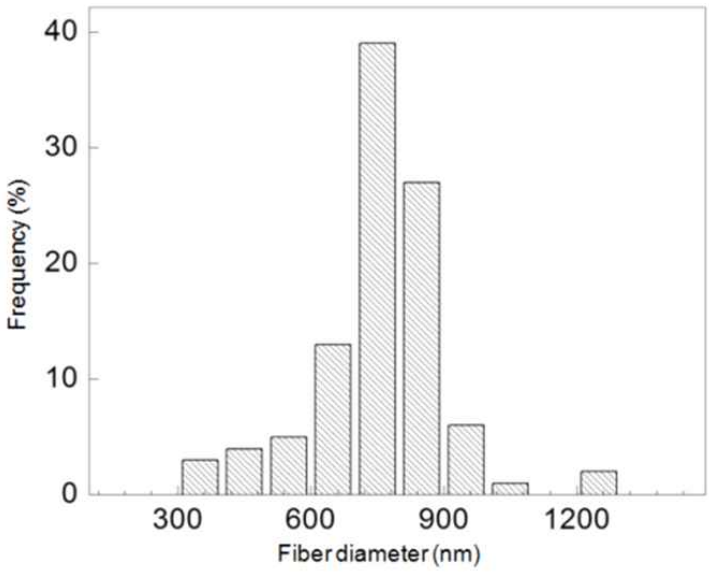

Figure 3.16. Diameter distribution of PVDF-TrFE electrospun nanofibers

The AFM image figure 3.17 shows the morphology of bottom electrospun fiber on the metal electrode. The average diameter of bottom electrospun fibers (1100 nm) is longer than that of the top electrospun fibers (750 nm) and an AFM height profile shows that fiber width (1200 nm) was longer than height (700 nm) [Figure 3.18]. A fiber height profile that is spreaded nanochannel in shape implies strong impingement and a partially solidified fiber on the electrode.[61,62]

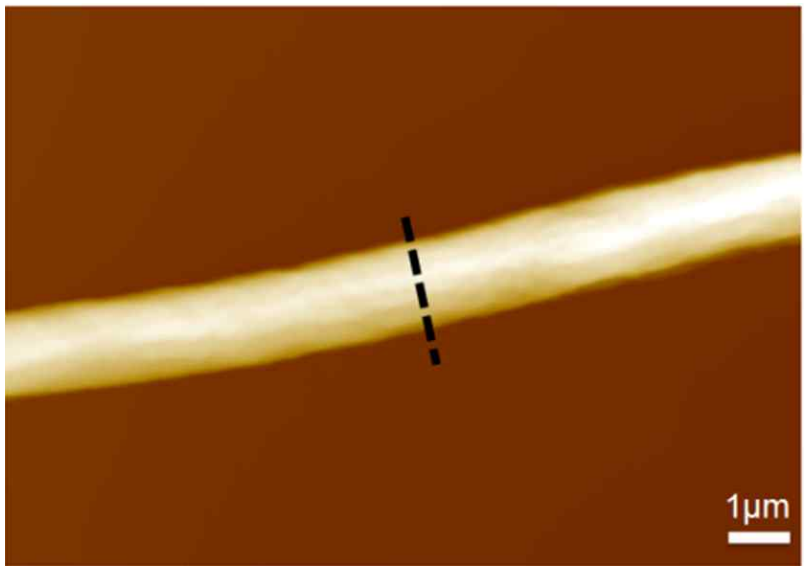

Figure 3.17. AFM image of a bottom PVDF-TrFE electrospun nanofibers.

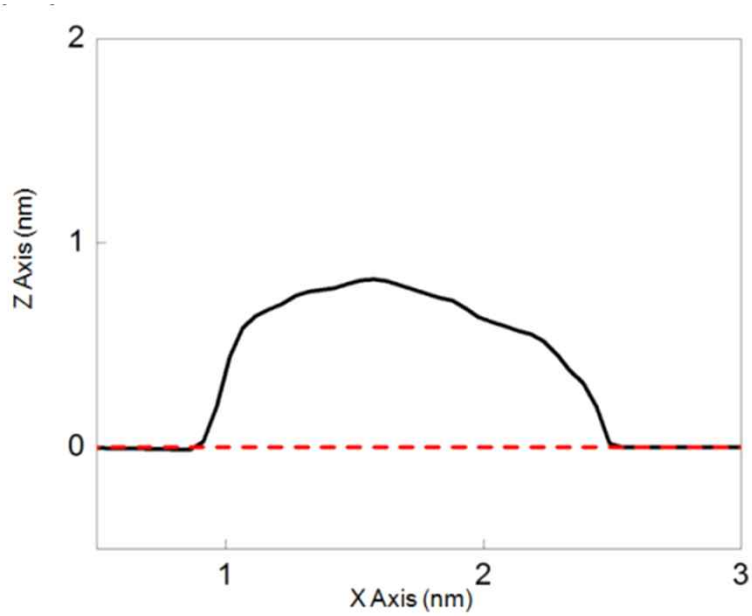

Figure 3.18. Height profile of bottom a PVDF-TrFE electrospun nanofibers.

When charged electrospun fibers are near the electrode, the residual charges in fiber induce electrons in the electrode and a local electric field is formed between the fiber and electrode. In this situation, a portion of the charge in the fiber is dissipated but some residual charges still remain.[63] The external electric field is reduced by accumulating charged fiber on the electrode but the change in external electric field is not high.

Simulation results showed that the local electric field decreased with the thickness of electrospun mat and increased with residual charge density.(Figure 3.19) Under certain condition, the electric field strength is higher than 10 MV/m which is sufficient for poling the polymer fibers. These results indicate that the electrical poling process was possible by residual charge and the electrospinning condition can affect the polarization and piezoelectric response of a piezoelectric polymer.

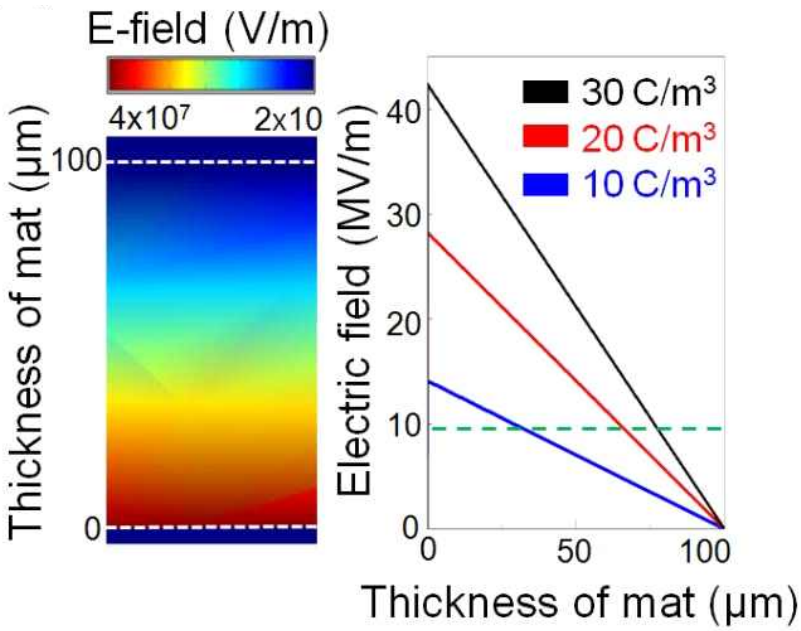

Figure 3.19. Simulation results of the local electric field by residual charge in the electrospun nanofibers.

The XRD pattern figure 3.20 is related to the crystal structure and the peak intensity ratio indicates the relative α- and β-phase ratio of PVDF-TrFE. It found the two obvious diffraction peaks at 2Θ = 18.4° and 20.2° corresponding to the reflections of the (020) plane of the a-phase and the (110) plane of the β-phase, respectively. In the electrospun fibers, the peak at 2Θ = 18.4° was significantly decrease compared to that of casting film, confirming that mechanical stretching occurs and a nonpolar α-phase structure is transformed to a polar β-phase structure by electrospinning. Also, the XRD patterns of the top and bottom electrospun fibers were similar. The XRD results indicated that content of the β-phase structure of bottom electrospun fibers was similar with that of top electrospun fibers.

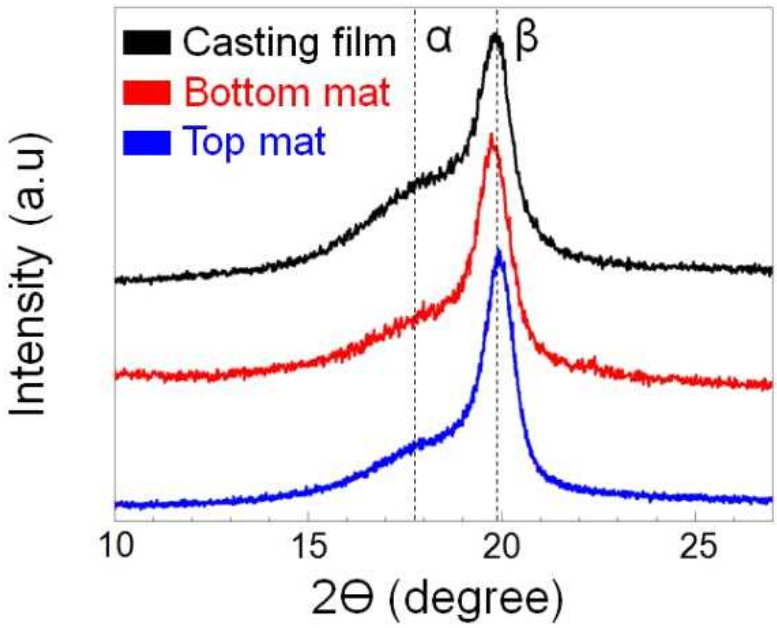

Figure 3.20. XRD pattern of electrospun PVDF-TrFE fibers.

The open circuit voltages of the top and bottom electrospun mat are compared in Figure 3.21. During repeat cycles, the voltage was positive at the

pressure state and negative at the release state. The average peak voltage output of the bottom electrospun mat was 1.81 V and that of the top electrospun mat was 0.38 V, where impact speed was 30 mm/s and pressure was 0.24 MPa.

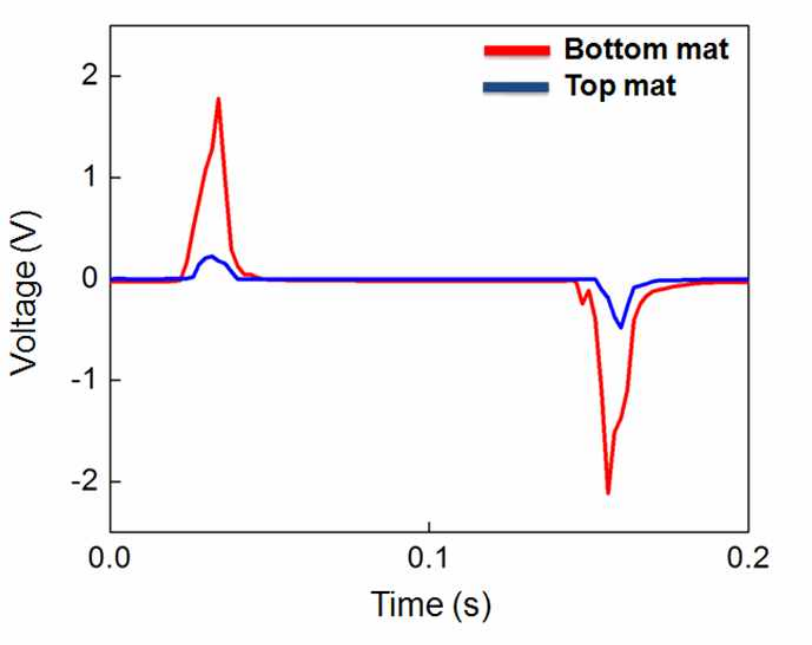

Figure 3.21. Piezoelectric voltages of electrospun PVDF-TrFE nanofibers at one cycle.

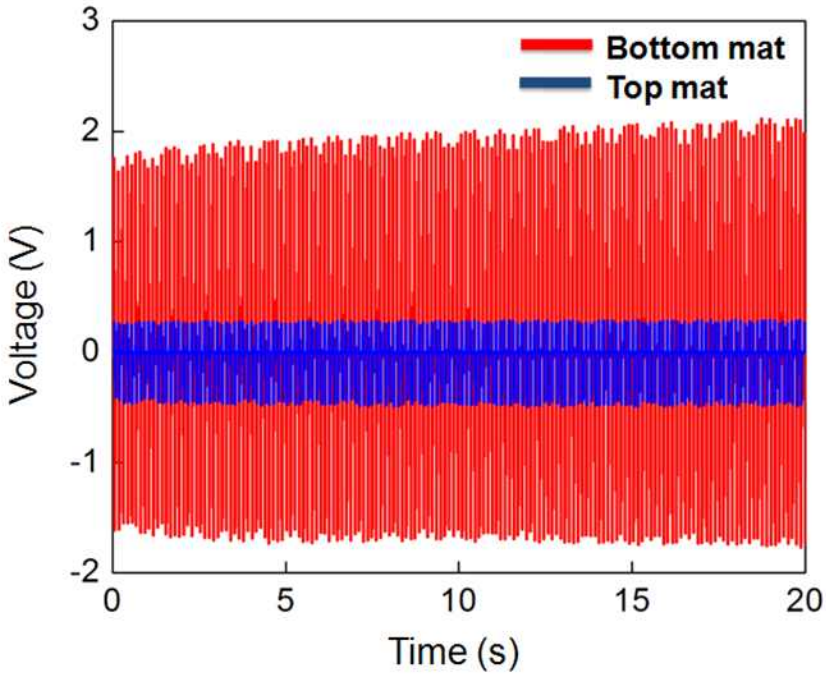

Figure 3.22. Piezoelectric voltages of electrospun PVDF-TrFE fibers at repeat cycle.

The main origins of piezoelectric responses can be divided into to two factors; one is beta phase ratio and the other is molecular dipole alignment in the electrospun fibers. As shown the XRD results, it confirmed that the β-phase structure ratio of bottom electrospun fibers was similar with that of top electrospun fibers, and thus the piezoelectric voltage outputs imply the molecular dipoles alignment of electrospun fibers. The results suggested that the molecular dipoles alignment of bottom electrospun mat was higher than that of top electrospun mat and show a similar tendency with the simulation. It can be concluded that an additional poling process by local electric field from residual charge occurred during electrospinning.

Wearable energy harvesting technologies must consider flexibility and stretchability, to ensure comfortable wearing. Stretchable piezoelectric electrospun fibers were fabricated by electrospinning a solution containing $BaTiO_3$ and SEBS. $BaTiO_3$/SEBS electrospun fibers with an average thickness of 100 μm were able to stretch up to 200% and showed superior mechanical stability over 200 repetitive stretching cycles. $BaTiO_3$ is an excellent electronic ceramic and has a high dielectric constant at room temperature, which makes it a suitable material for ceramic capacitors in many electronic devices. SEBS with superior tensile strength and elongation has been used to improve the compatibility and toughness of the components of composite. Figure 3.23 shows the $BaTiO_3$/SEBS electrospun fibers.

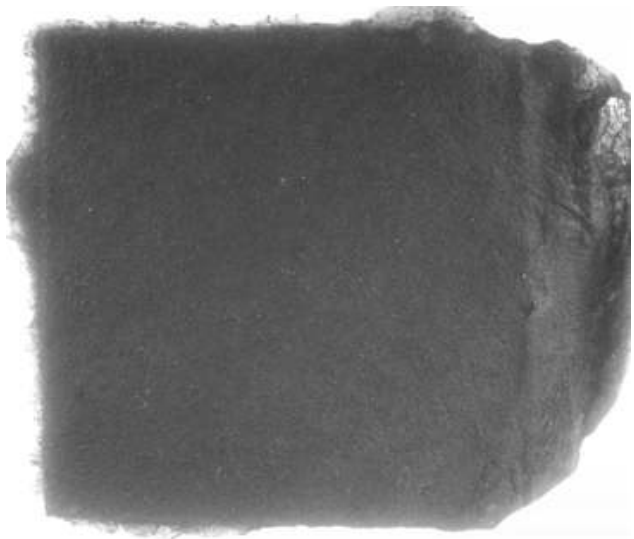

Figure 3.23. $BaTiO_3$/SEBS electrospun nanofibers.

Figure 3.24 shows the original state, stretching state, and released state of the $BaTiO_3$/SEBS electrospun fibers. In order to obtain an optimum stretching rate, all $BaTiO_3$/SEBS electrospun were uniaxially stretched at different strain rates beginning from 40 mm/s, using a stretching machine. The thickness of the $BaTiO_3$/SEBS electrospun fibers was 100μm. The fibers could be stretched

up to a maximum of 200% and showed superior mechanical stability over 200 stretching cycles. With this property, the $BaTiO_3$/SEBS electrospun fibers have the advantage of semipermanent and are applicable in various fields.

Figure 3.24. Optical images of $BaTiO_3$/SEBS electrospun fibers in original, stretched and released states.

Figure 3.25 shows an experiment conducted to verify the piezoelectric property, and its results. Under continuous pressing cycles, the $BaTiO_3$/SEBS electrospun fibers repeatedly generated a voltage of 6 V. During the stretching and releasing cycles, the $BaTiO_3$/SEBS electrospun fibers showed capability of producing stable power.

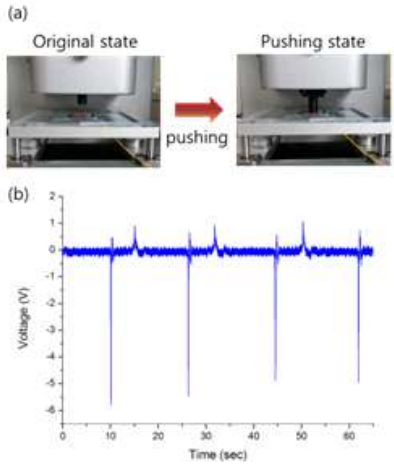

Figure 3.25. Piezoelectric voltage of $BaTiO_3$/SEBS electrospun nanofibers.

3.7 Conclusion

PVDF-TrFE electrospun fibers were fabricated by FFES and confirmed to have piezoelectric properties. The transition of the crystalline structure from α-phase to β-phase was similar for top and bottom electrospun fibers, as revealed by XRD analysis. However, the piezoelectric output of bottom electrospun mat was higher than that of top electrospun mat. The results are in agreement with the trend of the simulation that calculated the local electric field by the residual charge near the electrode. This suggest that the piezoelectric response increased as improved polarization by local electric field generated by residual charges, implying that the energy conversion efficiency of the electrospun fibers can be controlled by electrospinning conditions.

In summary, $BaTiO_3$/SEBS electrospun fibers can be manufactured using the electrospinning process. The maximum stretching in the $BaTiO_3$/SEBS electrospun fibers is close to double its original form. The electrical output of a $BaTiO_3$/SEBS electrospun fiber, obtained using a pushing machine, is 6 V. The $BaTiO_3$/SEBS electrospun fibers fibers manufactured in this study can be applied in flexible and stretchable generators for low-power supplies and in easy-to-move energy harvesters.

The PVDF-TrFE electrospun nanofibers and $BaTiO_3$/SEBS electrospun fibers suggest highly promising conversions of the mechanical movements generated during human activity into electricity. This innovative approach used in this study can inspire several research areas related to wearable electronics.

IV. Textile based Triboelectric Generator

4.1 Introduction

Energy harvesting technologies obtain electric energy from the ambient environment, e.g., solar[64], wind[65], thermal[66], and mechanical energy.[67-68] Energy harvesting has emerged as one of the most promising solutions for the rapidly increasing energy crises and global warming issues. Wearable energy-harvesting technologies are attractive for reducing the size and weight of electronic devices. Wearable energy sources should be flexible, lightweight, and ease to use. Wearable devices typically use conventional electrochemical batteries as energy sources. However, a battery does not provide energy consistently because it has a limited lifetime and is not durable. Recently, simple, highly efficient, and cost-effective triboelectric generators(TEGs) have been developed.[69-80] Among them, fiber/textile type TEG[81-87] technologies provide an energy source for self-powered devices, e.g., wearable devices, electronic skin, bio-medical devices, and portable electronics, because of their lightweight, flexibility, and comfort. In principle, triboelectric energy-harvesting technologies operate by contact electrification and electrostatic induction. As our body movements, e.g., stretching, pressing, and rubbing, are frequent and easily accessible mechanical-energy sources, textile-based TEGs integrated into clothing can effectively convert this mechanical energy into electrical energy. Most previously developed textile-based TEGs have generated energy based on pressing and rubbing motions.

In this study, this propose a corrugated textile-based triboelectric generator (CT-TEG), which generates energy not only by pressing and rubbing but also by stretching. The CT-TEG is sewn into a corrugated structure using the textile characteristics. As a result, the output voltage of the triboelectric

generator 30.3 V, 27.2 V, 3.8 V at stretching, pressing and rubbing motions, respectively. Also, the CT-TEG generated energy under mechanical deformation of wrist, arm and foot and light up 54 light emitting diodes connected in series. The proposed CT-TEG is an extremely promising power supply for wearable devices.

4.2 Theoretical Background of TEG

4.2.1 Triboelectricity and Static Electricity

Static electricity is generally produced by the contact between different materials. Materials are usually electrically neutral because they contain equal numbers of positive (+) charges and negative (−) charges. However, when two materials are in contact, or are separated, electrons move from one material to the other upon contact, leaving an excess of positive charge on one material and an excess of negative charge on the other, which is the cause of static electricity.

Studies have been conducted on the prevention of static electricity, which has been regarded as an obstacle to everyday life and the industry. Zhong Lin Wang's team at Georgia Tech, in 2012, reported a triboelectric nanogenerator that could effectively harvest energy using the static electricity property.

4.2.2 Triboelectric Series

Application of mechanical kinetic energy to two materials with different static electricity properties causes friction on the surface. One atom loses an electron and becomes positively charged, while another atom gains an electron and becomes negatively charged. If neutrally charged materials are subjected to friction, electrons move from one material to the other; thereby, one

material becomes positively charged while the other becomes negatively charged. The Triboelectric Series is a list of materials, showing the tendency of materials to lose or gain electrons.

Positive			Negative
	Polyformaldehyde 1.3-1.4	(continued)	
	Etylcellulose	Polyester (Dacron)	
	Polyamide 11	Polyisobutylene	
	Polyamide 6-6	Polyuretane flexible sponge	
	Melanime formol	Polyethylene Terephthalate	
	Wool, knitted	Polyvinyl butyral	
	Silk, woven	Polychlorobutadiene	
	Aluminum	Natural rubber	
	paper	Polyacrilonitrile	
	Cotton, woven	Acrylonitrile-vinyl chloride	
	Steel	Polybisphenol carbonate	
	Wood	Polychloroether	
	Hard rubber	Polyvinylidine chloride (Saran)	
	Nickel, copper	Polystyrene	
	Sulfur	Polyethylene	
	Brass, silver	Polypropylene	
	Acetate, Rayon	Polyimide (Kapton)	
	Polymethyl methacrylate (Lucite)	Polyvinyl Chloride (PVC)	
	Polyvinyl alcohol	Polydimethylsiloxane (PDMS)	
	(continued)	Polytetrafluoroethylene (Teflon)	

Positive			Negative
	Aniline-formol resin	Polyvinyl alcohol	
	Polyformaldehyde 1.3-1.4	Polyester (Dacron) (PET)	
	Etylcellulose	Polyisobutylene	
	Polyamide 11	Polyuretane flexible sponge	
	Polyamide 6-6	Polyethylene terephthalate	
	Melanime formol	Polyvinyl butyral	
	Wool, knitted	Formo-phenolique, hardened	
	Silk, woven	Polychlorobutadiene	
	Polyethylene glycol succinate	Butadiene-acrylonitrile copolymer	
	Cellulose	Nature rubber	
	Cellulose acetate	Polyacrilonitrile	
	Polyethylene glycol adipate	Acrylonitrile-vinyl chloride	
	Polydiallyl phthalate	Polybisphenol carbonate	
	Cellulose (regenerated) sponge	Polychloroether	
	Cotton, woven	Polyvinylidine chloride (Saran)	
	Polyurethane elastomer	Poly(2,6-dimethyl polyphenyleneoxide)	
	Styrene-acrylonitrile copolymer	Polystyrene	
	Styrene-butadiene copolymer	Polyethylene	
	Wood	Polypropylene	
	Hard rubber	Polydiphenyl propane carbonate	
	Acetate, Rayon	Polyimide (Kapton)	
	Polymethyl methacrylate (Lucite)	Polyethylene terephtalate	
	Polyvinyl alcohol	Polyvinyl Chloride (PVC)	
	(continued)	Polytrifluorochloroethylene	
		Polytetrafluoroethylene (Teflon)	

Figure 4.1. Triboelectric series.[88]

4.2.3 Fundamentals of Triboelectrification

Figure 4.2 shows a schematic diagram of triboelectric energy harvesting. [88] When two different materials are in contact, their surfaces become charged owing to friction. When these materials are separated, compensating charges accumulate on the upper and lower electrodes by electrostatic induction, and current flows through the outer electrode until the charges are balanced. When the two materials are brought close, the compensating charges disappear, and current flows in the opposite direction through the outer electrode. Such repeated contact and separation enables the current to flow between the electrodes.

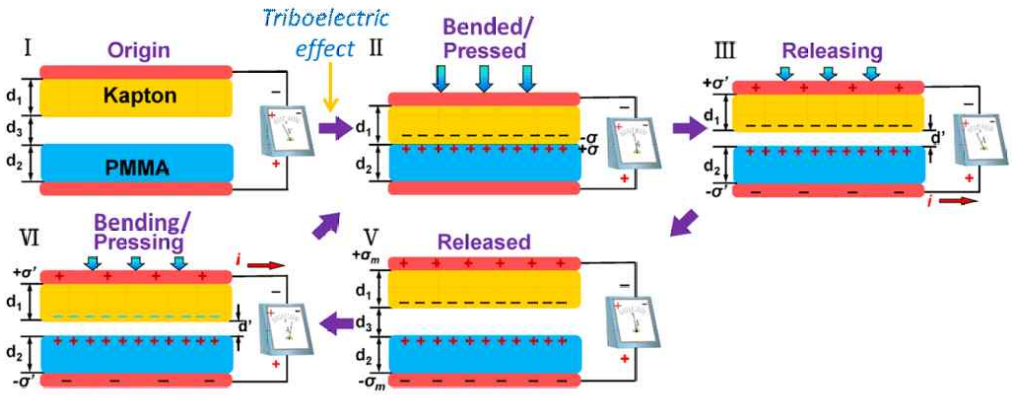

Figure 4.2. Vertical contact-separation mode of triboelectric nanogenerator.

4.2.4 Application of Triboelectric Generators

a. TENGs based Bulk-Scale Power Source

TENG-based bulk-scale power sources can be used for harvesting energy from water. The water-related energy sources such as ocean waves, rainwater, and water drops in the environment have abundant amounts of energy. They can be good alternatives to solar energy. [89]The contact electrification between water and polymer has been used to harvest wave energy and detect the alcohol concentration and temperature of water. [90]

Water-related TENGs are designed to harvest electrostatic energy from flowing water. The output power density is 11.56 mW/m^2. The TENG is integrated with window glass. When deionized water drops from the washing bottle impacts the TENGs on the window glass, outputs are generated. [91]

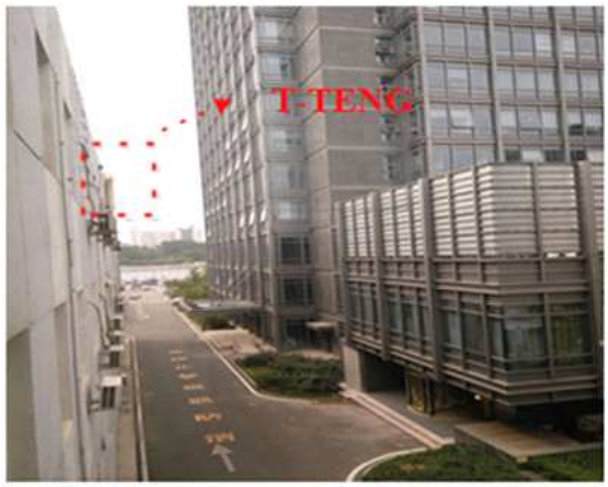

Figure 4.3. Application of water-related TENG.

b. TENGs based Micro/Nano-Scale Power Source

Micro/nano-scale TENGs are used to power wearable and small electronics. This requires not only miniaturization of the various electronic

components but also, and more importantly, their incorporation into fabrics or their implantation in the human body. [92-93] Recently, simple and small TENGs have been successfully developed and used to harvest mechanical energy. [94] Lightweight, flexible, and stretchable TENGs, in particular, are critical challenges in the field of wearable electronics.

Figure 4.4 shows the structure of a flexible triboelectric generator. Polymer-based TENGs are flexible and simple and can convert random mechanical energy in our living environment into electricity. These technologies have great potential for powering mobile and personal electronics in self-powered systems and medical applications. [95]

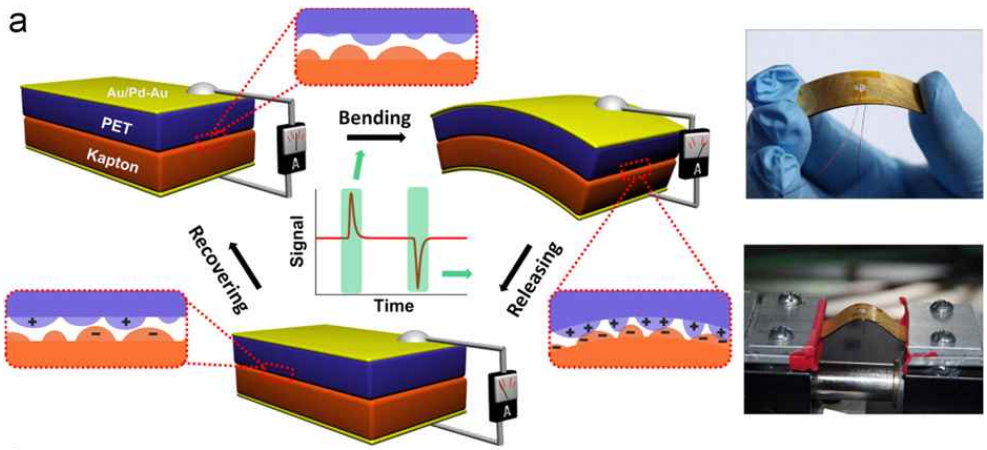

Figure 4.4. Flexible triboelectric generator.

Textile-based TENGs are attractive because of their excellent flexibility, light weight, and comfort. They are widely applied in wearable electronic devices. Figure 4.5 shows a nanopatterned textile-based triboelectric generator. Silver (Ag)-coated textile and polydimethylsiloxane (PDMS) nanopatterns based on ZnO nanorods are formed on an Ag-coated textile template. The output voltage and output current are approximately 120 V and 65 μA, respectively. [96]

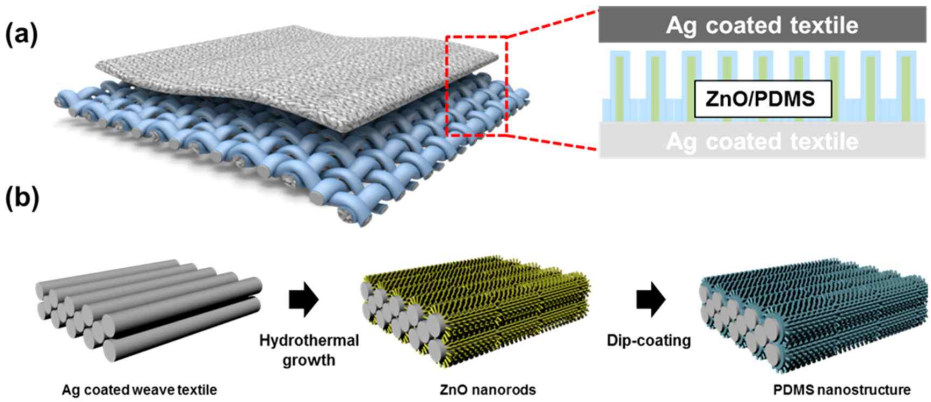

Figure 4.5. Textile type triboelectric generator.

c. Sensor applications of the TENG

Simple, flexible, and cost-effective TENGs available advantages with practical applications. The recent developments in TENGs, as a new technology for mechanical energy harvesting, can be utilized in self-powered active mechanical sensors because the generated electrical signals are determined by the input mechanical behaviors.

Figure 4.6 shows an acceleration sensor that can measure the acceleration using a triboelectric generator. Based on the coupling of triboelectric and electrostatic effects, a potential difference proportional to the mass displacement is generated between the two aluminum electrodes. [97]

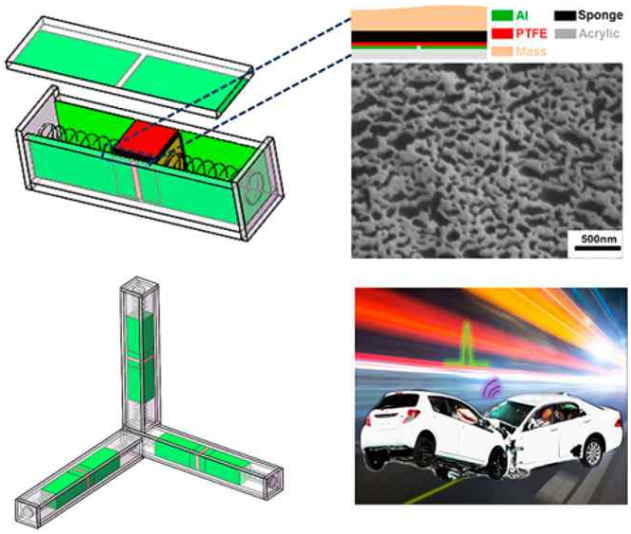

Figure 4.6. Triboelectric generator based acceleration sensor.

Figure 4.7 shows a self-powered thin-film motion vector sensor. It is a robust and self-powered kinematic vector sensor. The device derives its operational energy from the close-proximity triboelectrification of two surfaces. [98]

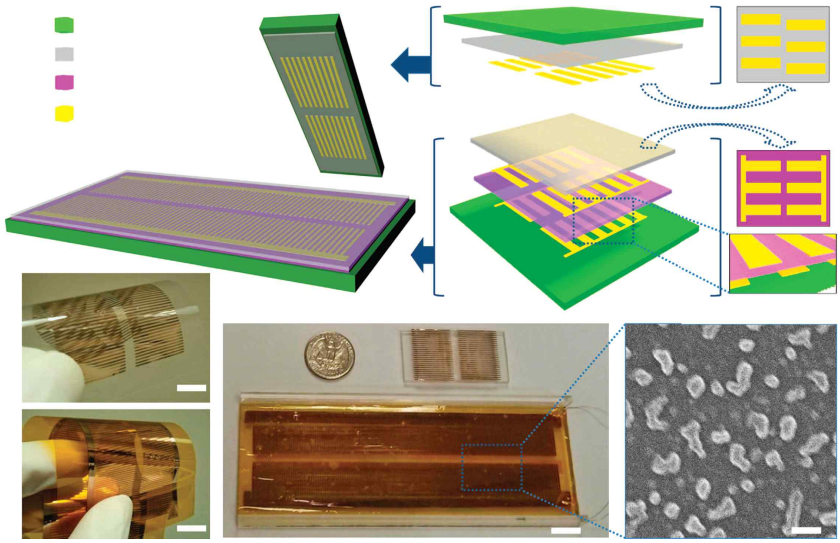

Figure 4.7. Schematic and experimental structure of a TENG.

Figure 4.8 shows a self-powered tactile sensing system based on the TENG. [99] It can respond to the contact electrification caused by an external physical trigger. The TENG sensor uses polymer nanowires on the contact surface, and demonstrates a high pressure sensitivity of 44 mV Pa^{-1}.

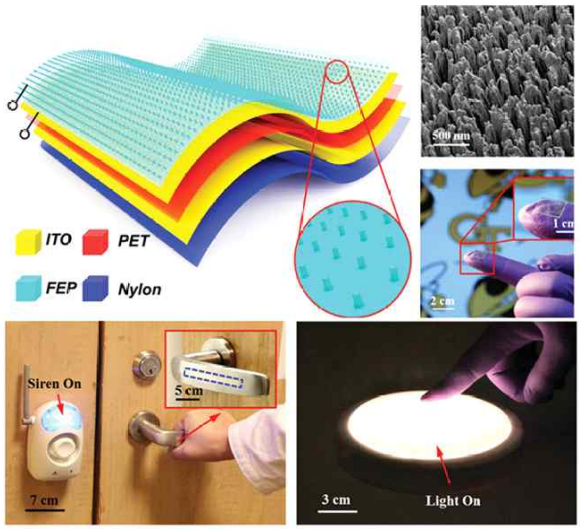

Figure 4.8. Self-powered, ultrasensitive, flexible tactile sensor.

Bai et al. proposed a TENG sensor targeting pressure change detection (shown in Figure 4.9). [100] It was found that the sensor exhibited high resolutions of 0.34 Pa and 0.16 Pa when the air pressure increased and decreased, respectively. The TENG demonstrated applications in devices used for sensing footsteps, respiration, or heartbeat.

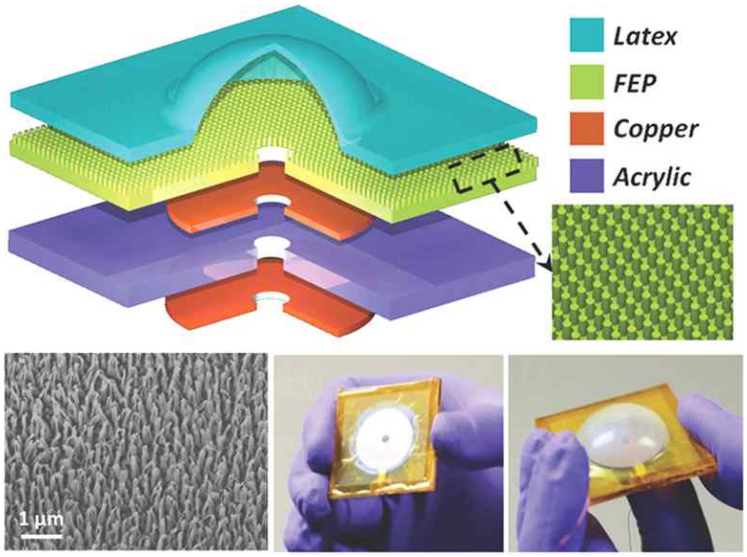

Figure 4.9. Membrane-based self-powered sensor.

Li et al. proposed powering pacemakers using breathing-driven implanted TENGs. The authors demonstrated that the energy generated from breathing could be directly harnessed by the TENG to power a prototype pacemaker.

4.3 Structural Design

The design of the CT-TEG is schematically shown in Figure 4.10. To analyze the electrical characterization, the top and bottom electrodes of the TEG are connected to the Ag textile. The Ag textile was selected as the electrode because of its lightweight and good stretchability. The fabricated CT-TEG consists of top and bottom layers, which are silk/Ag textile and silicon (Si)-rubber/Ag textile, respectively. The silk and Si-rubber are used as positive and negative triboelectric active materials. The bottom layer is composed of Si-rubber coated on a Ag textile substrate, which is then left at room temperature for 3 h. The top layer is composed of a corrugated stretchable Ag/silk textile sewn to the bottom layer.

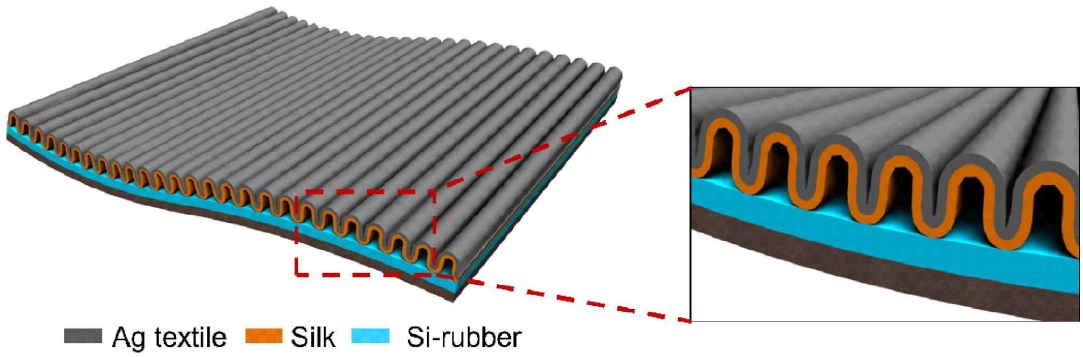

Figure 4.10. Schematic illustration of the corrugated textile-based triboelectric generator.

Figure 4.11 is a cross-sectional scanning electron microscope (SEM) image of the Si-rubber-coated Ag textile as bottom layer. The exposed Si-rubber is clear coated on the Ag textile substrate. The thickness of Si-rubber layer is about 223 μm.

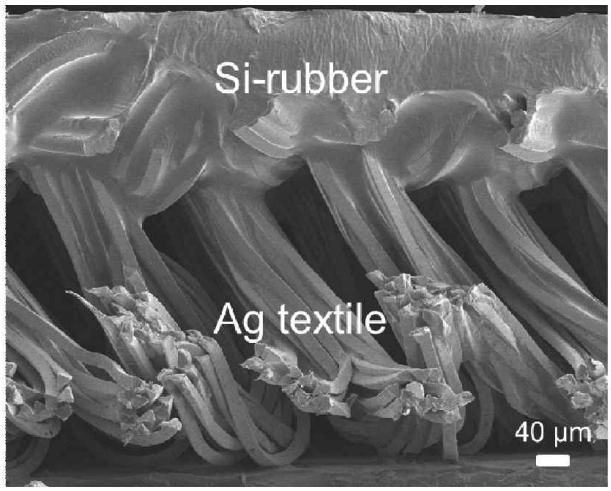

Figure 4.11. Cross-sectional SEM image of the Si-rubber-coated Ag textile.

The SEM images of woven conductive textile and knitted conductive textile shown in Figure 4.12 and 4.13, respectively. Figure 4.14 is the SEM image of the silk textile as the top layer. The surface of the silk textile has roughness, which leads to efficient friction. The average diameters of the silk textile were 16 μm.

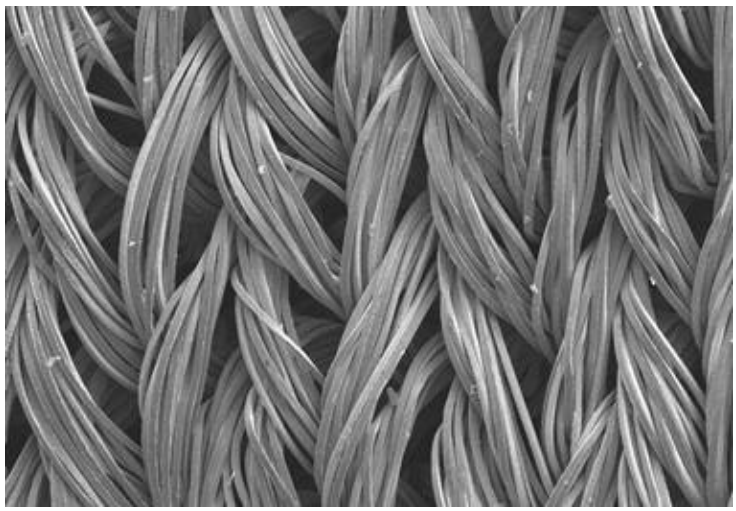

Figure 4.12. SEM image of woven conductive textile.

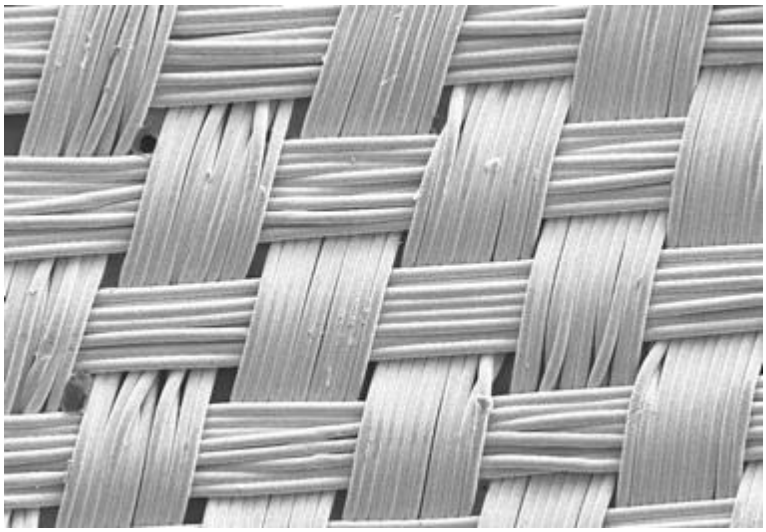

Figure 4.13. SEM image of knitted conductive textile.

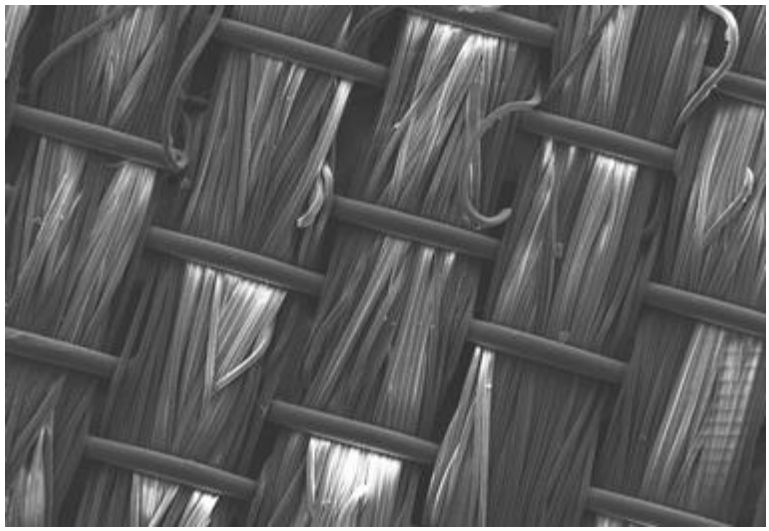

Figure 4.14. SEM image of silk textile.

A photograph of a fabricated TEG is shown in Figure 4.15. The CT-TEG has a naturally formed air gap from the corrugated structure without additional spacers, e.g., springs or sponges. Figure 4.15(right) is a photograph of the CT-TEG in the stretched state. The CT-TEG can be stretched up to 140%.

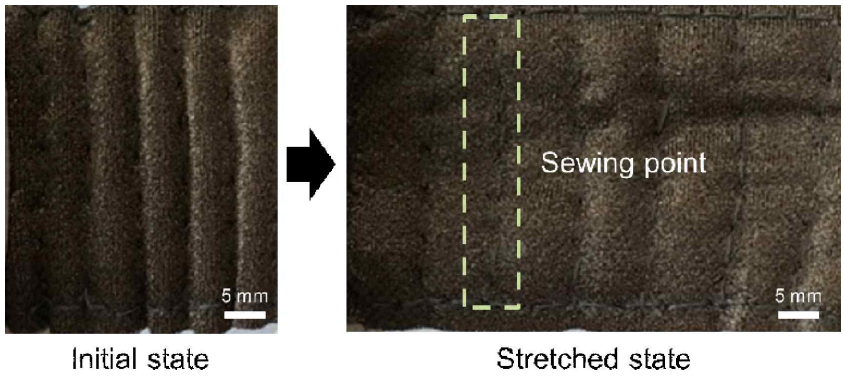

Figure 4.15. Corrugated structure of a textile-based triboelectric generator (left) orrugated textile-based triboelectric generator in the stretched state(right).

4.4 Operating Mechanism

The power-generation mechanism of the CT-TEG is illustrated in Figure 4.16. The CT-TEG enables energy generation by a conjunction of triboelectrification and electrostatic induction. Since the silk and Si-rubber have different electron-attracting abilities, a surface charge is transferred when the two are brought into contact. In the initial state, without any motion, no charge is transferred (Figure 4.16(i)). Once the CT-TEG is stretched, the TEG brings the silk and Si-rubber into full contact (Figure 4.16(ii)). Any motion will lead to a contact or separation between the silk and Si-rubber. The silk is charged positively and the Si-rubber is charged negatively because of their triboelectric characteristics. Because Si-rubber has a higher surface-electron affinity than the silk, the result is a net negative charge on the Si-rubber and a net positive charge on the silk.[66] Removing the external force causes a separation. Electrons flow from the Si-rubber-coated Ag-textile electrode to the silk/Ag-textile electrode (Figure 4.16(iii)). When the silk and Si-rubber are separated by the maximum distance, an electrical equilibrium is formed (Figure 4.16(iv)). When external force is applied to bring the silk and

Si-rubber into contact, it causes electrons to flow from the silk/Ag-textile electrode to the Si-rubber-coated Ag-textile electrode (Figure 4.16(v)). With the stretching, pressing, and rubbing motions, the surfaces of the silk and Si-rubber come into contact and rub against each other; thus, triboelectric charges are generated and distributed over the surface.

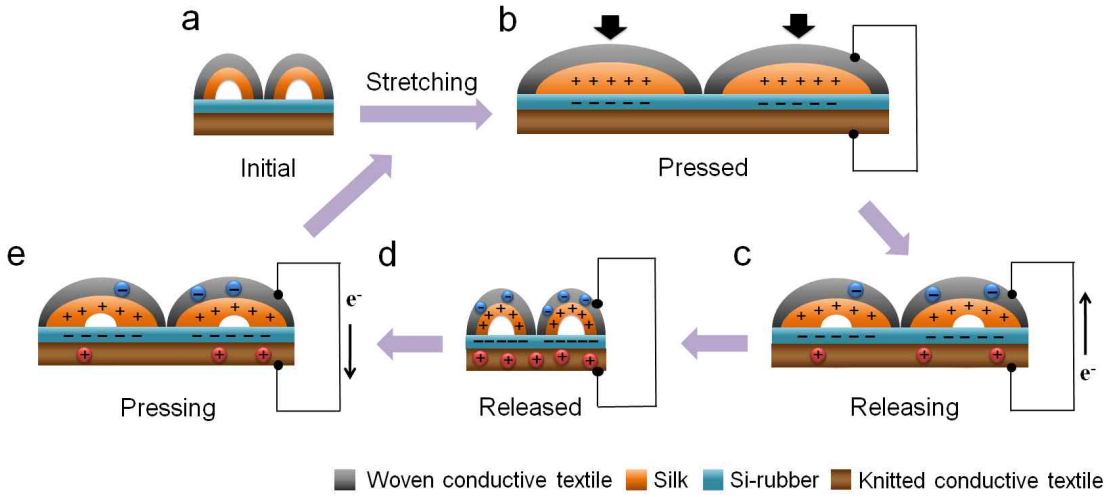

Figure 4.16. Schematic illustration showing the suggested working principle of the corrugated textile-based triboelectric generator.

4.5 Experiment

4.5.1 Fabrication of the CT-TEG

The CT-TEG consists of components such as Si-rubber and Silk, which are produced using the following methods. First, the production of Si-rubber involves mixing EcoFlex0050 solution in a one-to-one ratio for 15min using a glass stick. This cast the well-mixed Si-rubber solution on top of Ag-coated woven textile. It dry the thinly spread Si-rubber solution at room temperature 3 h. The figure 4.17 shows Si-rubber coated woven textile. Si-rubber is coated on conductive textile to keep in place during stretching motion.

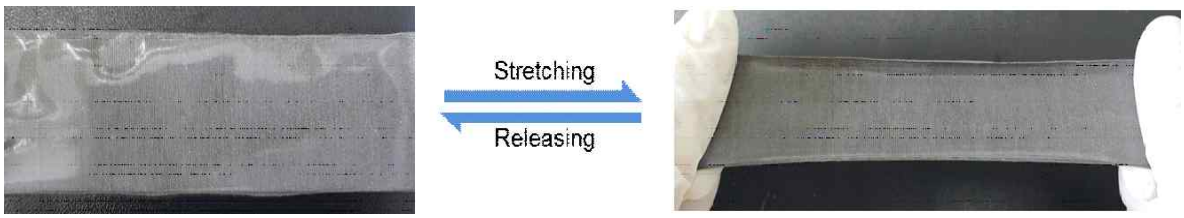

Figure 4.17. Original state of Si-rubber coated Ag textile(left) and stretching state of Si-rubber coated Ag textile(right).

Proposed CT-TEG was composed of corrugated stretchable conductive textile sewing on Ag textile which is coated by Si-rubber. The figure shows process of CT-TEG structure. The size of the CT-TEG was 5 cm x 3 cm.

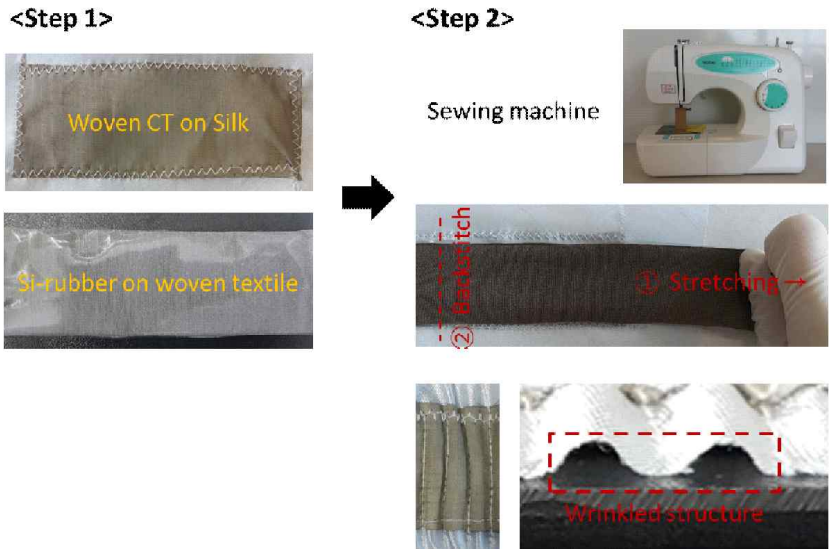

Figure 4.18 Process of corrugated textile based triboelectric generator.

4.6 Results

4.6.1 Factors Determining the Output Performance

Since triboelectrification is a surface charging effect, the surface morphology and friction materials will essentially determine the output of TENGs.[71] During the friction, the micro-structures provide larger triboelectric charges at the surface. When the two triboelectric charged layers are separated with an air gap by such spacer. Unfortunately, the spacer requires complicated fabrication or additional processes.

The CT-TEG has implemented micro patterns onto the tribo-surfaces. The presented CT-TEG is sewn into a corrugated structure that achieves an effective air gap without additional spacers. The textile surface of woven fibers efficiently generating triboelectric flat on Si-rubber without any expensive and complex processes. When Si-rubber coated conductive textiles and silk were overlapped, the output voltage is obtained under external forces. Therefore the CT-TEG utilizes broad and diverse fields of our living environment.

4.6.2 A Variety of Output Performances

The CT-TEG was measured under different conditions (stretching, pressing, and rubbing) to analyze its electrical output voltage performance. As demonstrated in figure 4.19, the open-circuit voltage is 30.3 V for stretching and releasing motions at a speed of 0.2 m/s.

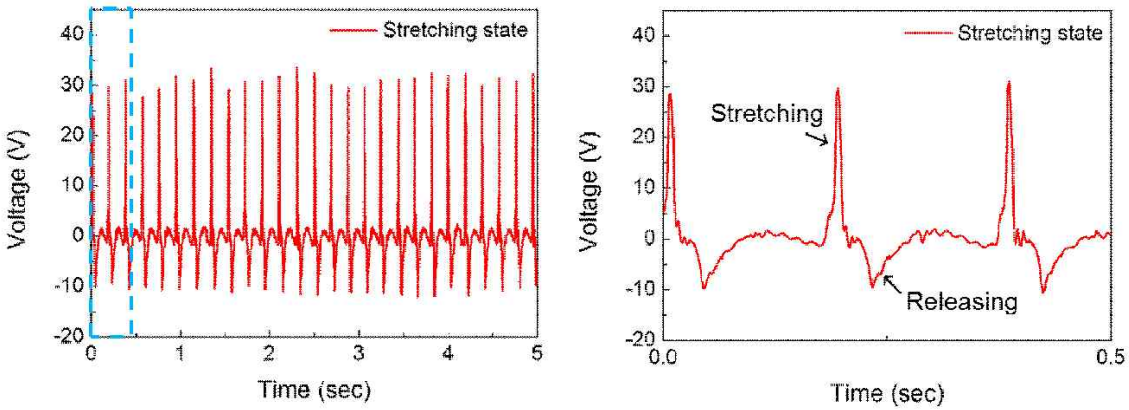

Figure 4.19. The output voltage at the stretched state.

Under vertical pressing forces of 1 kgf, the CT-TEG shows a repeatable and consistent electrical output of 27.2 V.

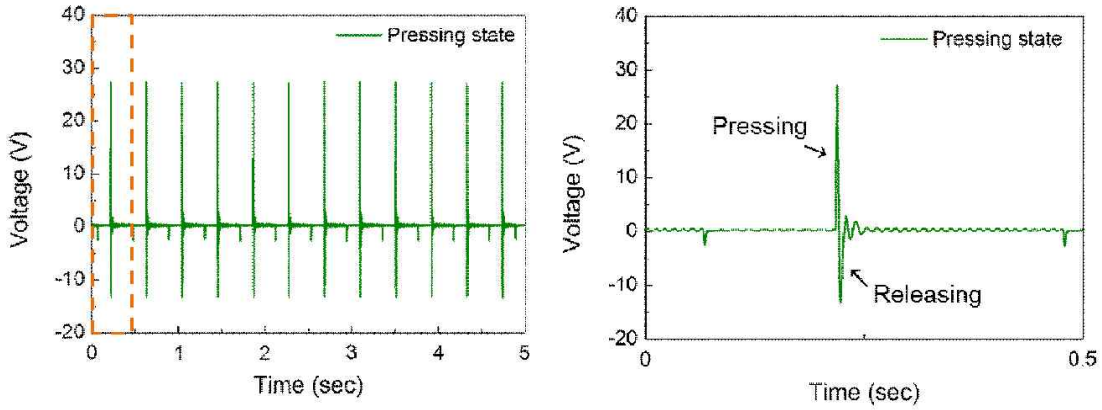

Figure 4.20. The output voltage at the pressing state.

The CT-TEG sliding mode operates at a frequency of 2 Hz; the electrical output shows 3.8 V. Thus, the corrugated structure of the CT-TEG generates power regardless of the motion.

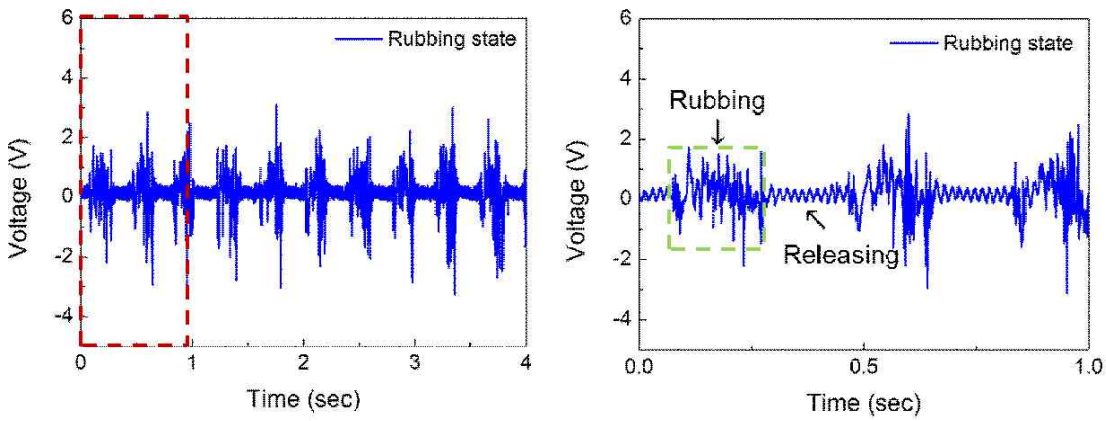

Figure 4.21. The output voltage at the rubbing state.

Also, the CT-TEG was measured under different conditions to analyze its electrical output current performance. As demonstrated in figure 4.21, the current is about 0.08 μA for stretching and releasing motions. Under vertical pressing forces of 1 kgf, the currnet of CT-TEG shows 0.09 μA.

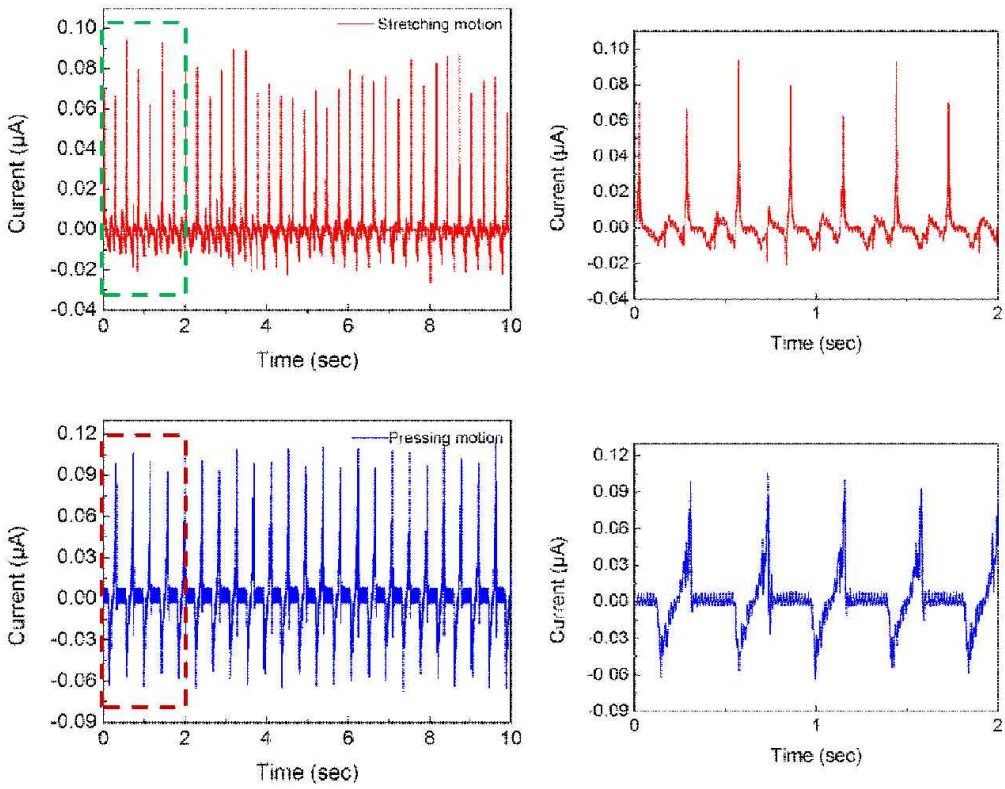

Figure 4.22. The output current at various mechanisms of the corrugated textile-based triboelectric generator. The output current at the stretched state and pressed state.

To investigate the effect of stretching frequency, it was varied from 2 to 4 Hz. It was evident that the voltages increased gradually with stretching frequency. At each frequency, the voltage values were obtained as follows: 7.45 V (2 Hz), 10.26 V (3 Hz), and 22.45 V (4 Hz).

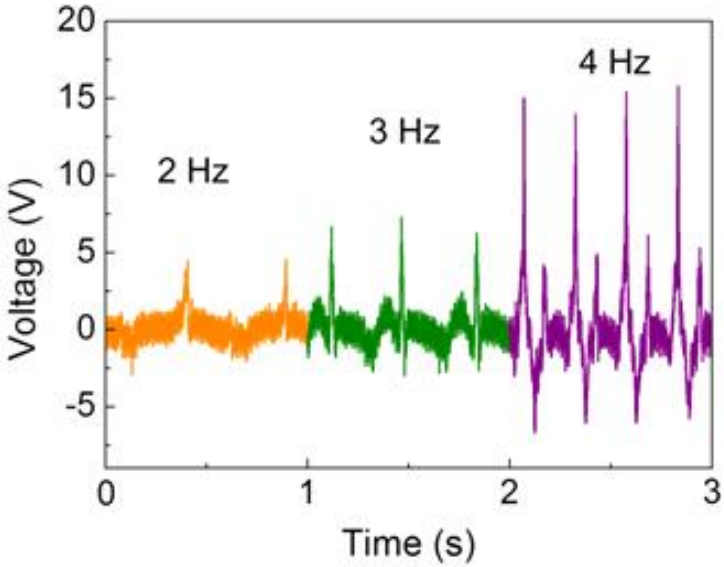

Figure 4.23 Output voltage for different stretching frequencies.

Figure 4.24 shows the output performance of the CT-TEG for stretching motion. The maximum output voltage increased with load resistance, whereas the maximum voltage decreased (Figure 4(a)). Accordingly, the instantaneous output power calculated using $W = I^2peak \times R$ was 16.6μW/cm^2 for a load resistance of 40Ω, as shown Figure 4.24(b). Figure 4.24(c) shows the output results vs. corrugated density. It is observed that the triboelectric output voltage increases with the corrugated density. Typically, a larger contact area produces more triboelectricity. The charging of capacitors with different capacitance values has been studied experimentally, as shown in Figure 4.24(d). It was observed that in the CT-TEG, the 1 μF capacitor charged to 114 mV in 20 s under periodic stretching and releasing. Additionally, the 2 μF capacitor charged to 99 mV. Therefore, the proposed CT-TEG is sufficient as an energy harvesting unit for a power source that employs stretching and releasing motions.

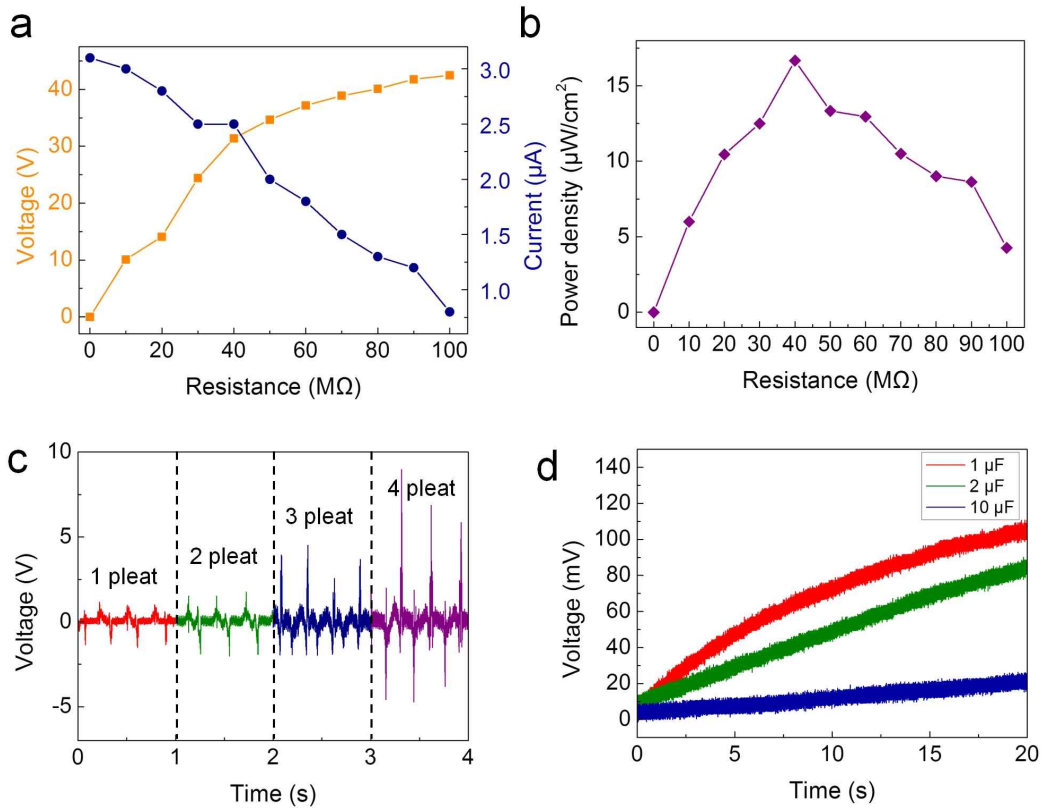

Figure 4.24 Output results of the CT-TEG for stretching motion.

To investigate the capability of the CT-TEG as a power source, we considered different parts of the human body. Here, the movement of the wrist, knee, and foot are the most important mechanical-energy sources supplied by the human body. As shown in Figure 4.25(a), a stretchable textile-based CT-TEG is placed over the wrist joint. The CT-TEG stretches when the wrist bends and relaxes when the wrist straightens, generating output voltage signals. The triboelectric voltage generated by the wrist joints is about 6.8 V. Figure 4.25(b) shows a corrugated textile-based CT-TEG attached to the side of the body to harvest energy from the arm rubbing. The output voltage is about 8.1 V. Figure 4.25(c) shows the corrugated textile-based CT-TEG generating energy from footsteps. Its output voltage is about 110.1 V, which is capable of lighting up about 54 light-emitting diodes

(LEDs) (Figure 4.26). Therefore, the proposed corrugated structure of the textile-based TEG has several advantages, e.g., harvesting different kinds of mechanical energy from the human body. It effectively converts ambient mechanical energy into electricity, which can be used to drive small electronics such as wearable devices.

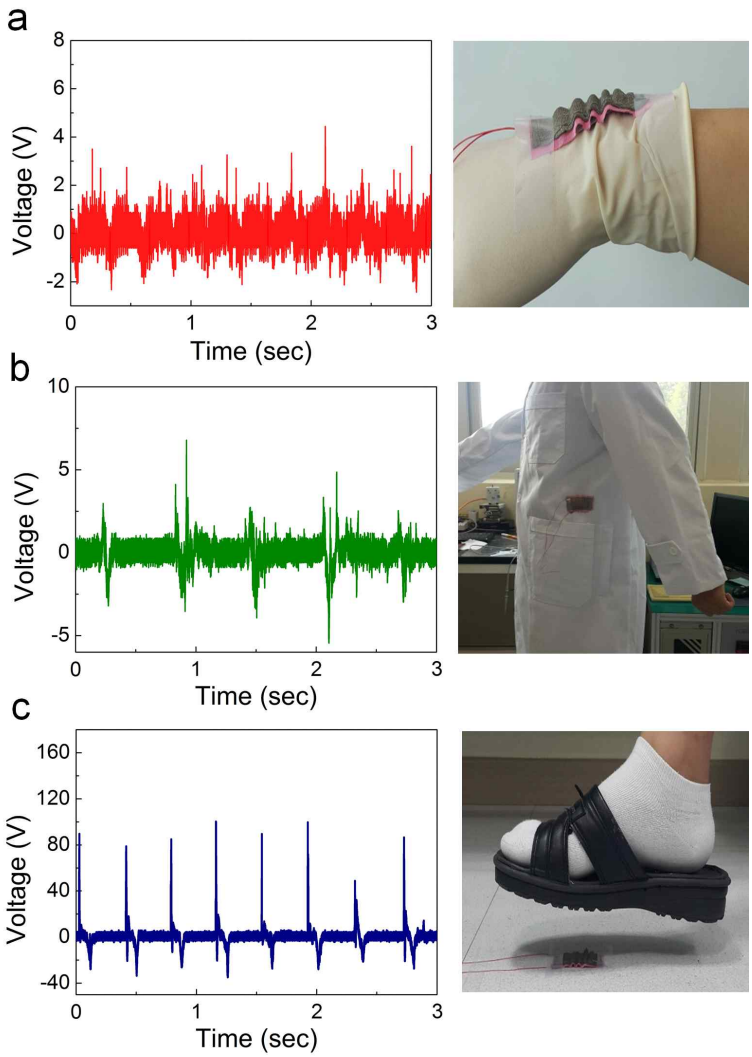

Figure 4.25. Application of a triboelectric generator. (a) Output voltage when bending and releasing the wrist. (b) Output voltage at the side of the body, harvesting energy from the arm rubbing. (c) Output voltage harvesting energy

from footsteps.

Its output voltage is about 90.1 V, which is capable of lighting up about 54 light-emitting diodes (LEDs) (Figure 4.26). Therefore, the proposed corrugated structure of the textile-based TEG has several advantages, e.g., harvesting different kinds of mechanical energy from the human body. It effectively converts ambient mechanical energy into electricity, which can be used to drive small electronics such as wearable devices.

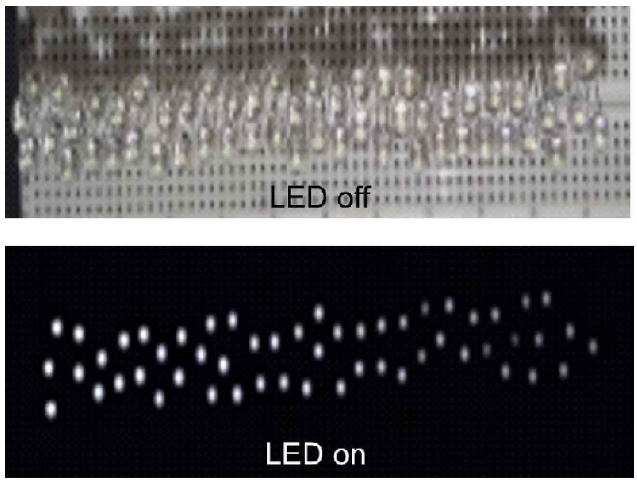

Figure 4.26. LED before and after lighting up.

In this study, this proposes a new corrugated structure for a textile-based triboelectric generator that can be attached to the surface of the human body to harvest mechanical energy. The fabric of the presented triboelectric generator is sewn into a corrugated structure that achieves an effective air gap without additional spacers. The maximum output voltages of the triboelectric generator are 30.3 V, 27.2 V, and 3.8 V for stretching, pressing, and rubbing motions, respectively.

Additionally, this demonstrated the generation of sufficient energy from various activities of the human body to operate 54 LED bulbs. It is expected that the stretchable and high-performing corrugated textile-based TEG can be widely used for wearable energy-harvesting systems.

4.7 Conclusion

In this study, this proposes a new corrugated structure for a textile-based triboelectric generator that can be attached to the surface of the human body to harvest mechanical energy. The fabric of the presented triboelectric generator is sewn into a corrugated structure that achieves an effective air gap without additional spacers. The maximum output voltages of the triboelectric generator are 30.3 V, 27.2 V, and 3.8 V for stretching, pressing, and rubbing motions, respectively.

Additionally, this demonstrated the generation of sufficient energy from various activities of the human body to operate 54 LED bulbs. It is expected that the stretchable and high-performing corrugated textile-based TEG can be widely used for wearable energy-harvesting systems.

Reference

[1] S. Roundy, P. K. Wright, J. Rabaey, “A study of low level vibrations as a power source for wireless sensor nodes", Computer Communications, vol. 26, pp. 1131-1144, July 2003.

[2] C.B. Williams, R.B. Yates, "Analysis of a micro-electric generator for microsystems", Sensors and Actuators A: Physical, vol. 52, pp. 8-11, March 1996.

[3] P. Glynne-Jones, J. Tudor, S.P. Beeby, N.M. White, "An electromagnetic, vibration-powered generator for intelligent sensor systems", Sensors and Actuators A: Physical, vol. 110, pp. 344-349, February 2004.

[4] D. Arnold, Review of microscale magnetic power generation. IEEE Transactions on Magnetics, vol. 43, pp. 940-3951, November 2007.

[5] P. D. Mitcheson, P. Miao, B. Start, E. Yeatman, A. Holmes, T. Green, "MEMS electrostatic micropower generator for low frequency operation", Sensors and Actuators A: Physical, vol. 115, pp. 523-529, September 2004.

[6] Y. B. Jeon, R. Sood, J.H. Jeongand, S. Kim, "MEMS power generator with transverse mode thin film PZT" Sensors and Actuators A: Physical, vol. 122, pp. 16-22, July 2005.

[7] W. J. Choi, Y. Jeon, J.H. Jeong, R. Sood, S.G. Kim, "Energy harvesting MEMS device based on thin film piezoelectric cantilevers" Journal of Electroceramics, vol. 17, pp. 543-548, November 2005.

[8] Y. Khan, A. E. Ostfeld, C. M. Lochner, A. Pierre and A. C. Arias, "Monitoring of vital signs with flexible and wearable medical devices" Advanced Materials, vol. 28, pp. 4373-7395, February 2005.

[9] S. J. Kim, J, H, We and B. J. Cho, "A wearable thermoelectric generator fabricated on a glass fabric", Energy & Environmental Science, vol. 7, pp. 1959-1965, March 2014.

[10] M. K. Kim, M. S. Kim, S. Lee, C. Kim and Y. J. Kim, "Wearable thermoelectric generator for harvesting human body heat energy", Smart Materials and Structures, vol. 23, pp. 105002-105008, September 2014.

[11] J. H. We, S. J. Kim and B. J. Cho, "Hybrid composite of screen-printed inorganic thermoelectric film and organic conducting polymer for flexible thermoelectric power generator", Energy, vol. 73, pp. 506-512, August 2014.

[12] C. Dun, C. A. Hewitt, H. Huang, D. S. Montgomery, J. Xu and D. L. Carroll, "Flexible thermoelectric fabrics based on self-assembled tellurium nanorods with a large power factor", Physical Chemistry Chemical Physics, vol. 17, pp. 8591-8595, November, 2015.

[13] S. L. Kim, K. Choi, A. Tazebay and C. Yu, "Flexible power fabrics made of carbon nanotubes for harvesting thermoelectricity", ACS Nano, vol. 8, pp. 2377-2386, February 2014.

[14] M. Van Bavel, V. Leonov, R. F. Yazicioglu, T. Torfs, C. Van Hoof, N. E. Posthuma, R. J. Vullers, "Wearable battery-free wireless 2-channel EEG systems powered by energy scavengers", Sensors & Transducers Journal, vol. 94, pp. 103-115, July 2008.

[15] T. Torfs, V. Leonov, R. J. Vullers, "Pulse oximeter fully powered by human body heat", Sensors & Transducers Journal, vol. 80, pp. 1230-1238, June 2007.

[16] Y. Qi, N. T. Jafferis, K. Lyons, C. M. Lee, H. Ahmad, M. C. McAlpine, "Piezoelectric Ribbons Printed onto Rubber for Flexible Energy Conversion", Nano Lett., vol. 10, pp. 524-528, January 2010.

[17] W. Wu, S. Bai, M. Yuan, Y. Qin, Z. L. Wang, T. Jing, “Lead Zirconate Titanate Nanowire Textile Nanogenerator for Wearable Energy-Harvesting and Self-Powered Devices”, ACS Nano, vol. 6, pp. 6231-6235, June 2012.

[18] W. S. Jung, M. J. Lee, M. G. Kang, H. G. Moon, S. J. Yoon, S. H. Baek, C. Y. Kang, “Powerful curved piezoelectric generator for wearable applications”, Nano Energy, vol. 13, pp. 174-181, April 2015

[19] S. Siddiqui, D. I. Kim, L. T. Duy, M. T. Nguyen, S. Muhammad, W. S. Yoon, N. E. Lee, “High-performance flexible lead-free nanocomposite piezoelectric nanogenerator for biomechanical energy harvesting and storage”, Nano Energy, vol. 15, pp. 177-185, July 2015

[20] J. Zhao, Z. You, “A shoe-embedded piezoelectric energy harvester for Wearable Sensors”, Sensors, vol. 14, pp. 12497-12510, July 2014

[21] Y.-K. Fuh, P.-C. Chen, Z.-M. Huang, H.-C. Ho, “Self-powered sensing elements based on direct-write, highly flexible piezoelectric polymeric nano/microfibers”, Nano Energy, vol. 11, pp. 671-677, January 2015

[22] S. Song, K.-S. Yun, “Design and characterization of scalable woven piezoelectric energy harvester for wearable applications”, Smart Mater. Struct., vol. 24, pp. 045008-045017, February 2015

[23] P. K. Yang, L. Lin, F. Yi, X. Li, K. C. Pradel, Y. Zi, C.-I. Wu, J.-H. He, Y. Zhang, Z. L. Wang, “A Flexible, Stretchable and Shape-Adaptive Approach for Versatile Energy Conversion and Self-Powered Biomedical Monitoring“ Advanced Materials, vol. 27, pp. 3817-3824, July 2015.

[24] T. Khan, A. E. Ostfeld, C. M. Lochner, A. Pierre and A. C. Arias, "Monitoring of vital signs with flexible and wearable medical devices", Advanced Materials, vol. 28, pp. 4373-4395, February 2016.

[25] X. Lu, P. Wang, D. Niyato, D. I. Kim and Z. Han, "Wireless charging

technologies: fundamentals, standards and network applications", IEEE Communications Surveys and Tutorials, to Appear, vol. 18, pp. 1413-1452, November 2015.

[26] J. Andrews, S. Venkatraman and C. Mrs.Sunitha, "Implementation of wireless body area networks in health monitoring", International Journal of Technical Research Applications, vol. 4, pp. 62-67, March 2016.

[27] M. J. Jeong, K. H. Park, J. M. Kim, J. H. Hwang, C. H. Hyoung and Y. T. Kim, A. Pierre and A. C. Arias, "Feasibility study on application of power transmission using magnetic coupling to body area network", Electoronics Letters, vol. 48, pp. 1013-1015, August 2012.

[28] Z. L. Wang and J. Song, "Piezoelectric nanogenerators based on zinc oxide nanowire arrays", Science, vol. 312, pp. 242-246, April 2006.

[29] K. Park, S. Xu, Y. Liu, G. Hwang, S. L. Kang, Z. L. Wang and K. J. Lee, "Pieozlectric BaTiO3 thin film nanovenerator on plastic substrates", Nano Letters, vol. 10, pp. 4939-4943, November 2010.

[30] W. Wu, S. Bai, M. Yuan, Y. Qin, Z. L. Wang and T. Jing, "Lead zirconate titanate nanowire textile nanogenerator for wearable energy-harvesting and self-powered devices", ACS Nano, vol. 6, pp. 6231-6235, June 2012.

[31] Y. Zhang, Y. Zhang, X. Xue, C. Cui, B. He, Y. Nie, P. Deng and Z. L. Wang, "PVDF-PZT nanocomposite film based self-charging power cell", Nanotechnology, vol. 25, pp. 105401-105407, February 2014.

[32] Y. H. Do, W. S. Jung, M. G. Kang, C. Y. Kang and S. J. Yoon, "Preparation on transparent flexible piezoelectric energy harvester based on PZT films by laser lift-off process", Sensor and Actuators, A: Physical, vol. 200, pp. 51-55, October 2013.

[33] Y. H. Do, W. S. Jung, M. G. Kang, C. Y. Kang, S. J. Yoon, "Preparation on transparent flexible piezoelectric energy harvester based on PZT films by laser lift-off process", Sensor and Actuators, A: Physical, vol. 200, pp. 51-55, October 2013.

[34] Y. H. Do, W. S. Jung, M. G. Kang, C. Y. Kang and S. J. Yoon, "Preparation on transparent flexible piezoelectric energy harvester based on PZT films by laser lift-off process", Sens. Actuators, A: Physical, vol. 200, pp. 51-55, October 2013.

[35] Q. Ahn, J. Y. Lim, S. M. Hong, J. Lee, J. Ha, H. J. Choi and Y. Seo, "Enhanced piezoelectric properties of electrospun poly(vinylidene fluoride)/multiwalled carbon nanotube composites due to high β phase formation in poly(vinyldene fluoride)", The Journal of Physical Chemistry, vol. 117, pp. 11791-11799, April 2013.

[36] L. F. Cui, Y. Yang, C. M. Hsu and Y. Cui, “Carbon–Silicon Core–Shell Nanowires as High Capacity Electrode for Lithium Ion Batteries”, Nano Lett. vol. 9, pp. 3370 – 3374, August 2009

[37] L. Ji, X. Zhang, “Electrospun carbon nanofibers containing silicon particles as an energy-storage medium”, Carbon 2009, vol. 47, pp. 3219 – 3226, November 2009

[38] J. J. Lee, E. W. Park, and S. H. Hyun, “Performance and Evaluation of Cu-.based Nano-.composite Anodes for Direct Utilisation of Hydrocarbon Fuels in SOFCs”, Fuel cells, vol. 10, pp. 145 – 155, February 2010

[39] S. Molla, V. Compari, “Polyvinyl alcohol nanofiber reinforced Nafion membranes for fuel cell applications” J. Membr. Sci. vol. 372, pp. 191 – 200, April 2011

[40] Z. Li, X. Cui, X. Zhang, Q. Wang, Y. Shao, Y. Lin, “Pt/carbon nanofiber nanocomposites as electrocatalysts for direct methanol fuel cells: Prominent

effects of carbon nanofiber nanostructures", Journal of nanoscience and nanotechnology, vol. 9, pp. 2316 - 2323, April 2009

[41] B.G. Choi, J. Hong, Y.C. Park, D.H. Jung, W.H. Hong, P.T. Hammond, H. Park, "Innovative polymer nanocomposite electrolytes: nanoscale manipulation of ion channels by functionalized graphenes" ACS Nano, vol. 5, pp. 5167 - 5174, May 2011

[42] S. Dong, X. Chen, L. Gu, L. Zhang, X. Zhou, Z. Liu, P. Han, H. Xu, J. Yao, X. Zhang, "A biocompatible titanium nitride nanorods derived nanostructured electrode for biosensing and bioelectrochemical energy conversion", Biosens. Bioelectron., vol. 26, pp. 4088 - 4094, June 2011

[43] J. Chang, M. Dommer, C. Chang, and L. Lin, "Piezoelectric nanofibers for energy scavenging applications", Nano Energy, vol. 1, pp. 356-371, May 2012.

[44] V. V. Kochervinskii, "Piezoelectricity in crystallizing ferroelectric polymers: Poly(vinylidene fluoride) and its copolymers(a review)", Crystallography Reports. vol. 48, pp. 649-675, July 2003.

[45] S. Egusa, Z.Wang, N. Chocat, Z.M. Ruff, A. M. Stolyarov, D. Shemuly, F. Sorin, P. T. Rakich, J. D. Joannopoulos and Y. Fink, "Matimaterial piezoelectric fibers", Nature materials, vol. 9, pp. 643-648, July 2010.

[46] M. S. Majdoub, P. Sharma, and T. Cagin, "Enhanced size-dependent piezoelectricity and elasticity in nanostructures due to the flexoelectric effect", Physical Review B, vol. 77, pp. 125424-125427, March 2008.

[47] C. Chang, V. H. Tran, J. Wang, Y. K. Fuh, and L. Lin, "Direct-write piezoelectric polymeric nanogenerator with high energy conversion efficiency", Nano Letters, vol. 10, pp. 726-731, January 2010.

[48] X. Chen, S. Xu, N. Yao and Y. Shi, "1.6 V nanogenerator for mechanical energy harvesting using PZT nanofibers", Nano Letters, vol. 10, pp. 2133-2137, May 2010.

[49] C. Chang, V. H. Tran, J. Wang, Y. K. Fuh, and L. Lin, "Direct-write piezoelectric polymeric nanogenerator with high energy conversion efficiency", Nano Letters, vol. 10, pp. 726-731, January 2010.

[50] T. Lei, L. Xu, Z. Zhan, J. Du, Y. Jiang, G. Zheng, L. Wang, and D. Sun, "Direct Fabrication of Polymer Nanofiber Membrane for piezoelectric Vibration Sensor : Sensors, Limerick, Ireland", IEEE Sensors, pp. 1367-1370, January 2012.

[51] D. Mandal, S. Yoon, and K. J. Kim, "Origin of piezoelectricity in an electrospun poly(vinylidenfluoride-trifluoroethylene) nanofber web-based nanogenerator and nano-pressure sensor", Macromolecular Rapid Communications, vol. 32, pp. 831-837, May 2011.

[52] D. Dhakras, V. Borkar, S. Ogale, and J. Jog, "Enhanced piezoresponse of electrospun PVDF mats with a touch of nickel chloride hexahydrate salt", Nanoscale, vol. 4, pp. 752-756, January 2012.

[53] J. Fang, X. Wang, and T. Lin, Electrical power generator from randomly oriented electrospun poly(vinylidene fluoride) nanofibre membranes", Journal of Materials Chemistry, vol. 21, pp. 11088-11091, June 2011.

[54] A. Baji, Y. W. Mai, Q. Li and Y. Liu, Electrospinning induced ferroelectricity in poly(vinylidene fluoride) fibers", Nanoscale, vol. 3, pp. 3068-3071, June 2011.

[55] J. S. Andrew and D. R. Clarke, "Effect of electrospinning on the ferroelectric phase content of polyvinylidene difluoride fibers", Langmuir, vol. 24, pp. 670-672, January 2008.

[56] J. Zheng, A. He, J. Li and C. C. Han, "Polymorphism Control of Poly(vinylidene fluoride) through Electrospinning", Macromolecular Rapid Communications, vol. 28, pp. 2159-2162, October 2007.

[57] G. Collins, J. Federici, Y. Imura, and L. H. Catalani, "Charge generation, charge transport, and residual charge in the electrospinning of polymers: A review of issues and complications", Journal of Applied Physics, vol. 111, pp. 044701, February 2012.

[58] J. Sakata and M. Mochizuki, "Preparation of organic thin films by an electrospray thenique I. crystal forms and their orientation in poly(vionylidene fluoride) films", Thin Solid Films, vol. 195, pp. 175-184, July 1990.

[59] I.B. Rietveld, K. Kobayashi, T. Honjo, K. Ishida, H. Yamada, and K. Matsushige, "Electrospray induced ferroelectricity in poly(vinylidene fluoride) thin films" Journal of Materials Chemistry, vol. 20, pp. 8272-8278, August 2010.

[60] L. H. Catalani, G. Collins, and M. Jaffe, "Evidence for molecular orientation and residual charge in the elctrospinning of poly(vutylene terephthalate) nanofibers", Macromolecules, vol. 40, pp. 1693-1697. February 2007.

[61] M. K. Shin, S. I. Kim, S. J. Kim, S. K. Kim, H. Lee, and G. M. Spinks, "Size-dependent elastic modulus of single electroactive polymer nanofibers", Applied Physics Letter, vol. 89, pp. 231929, December 2006.

[62] M. K. Shin, S. K. Kim, H. Lee, S. I. Kim and S. J. Kim, "The fabrication of polymeric nanochannels by electrospinning" Nanotechnology, vol. 14, pp. 195304-195307, April 2008.

[63] G. Collins, J. Federici, Y. Imura, and L. H. Catalani, "Charge generation, charge transport, and residual charge in the electrospinning of polymers: A

review of issues and complications", Journal of Applied Physics, vol. 111, pp. 044701, February 2012.

[64] M Sharma, A Chauhan, R Vaish and V. S. Chauhan "Finite element analysis on solar energy harvesting using ferroelectric polymer" Solar Energy, vol. 115, pp. 722-732, May 2015.

[65] M. Seol, J. Woo, S. Jeon, D. Kim, S. Kim, S. Park, J. and Hur, Y. Choi, "Vertically stacked thin triboelectric nanogenerator for wind energy harvesting" Nano Energy, vol. 14, pp. 201-208, May 2014.

[66] Y. Yang, W. Guo, K. Pradel, G. Zhu, Y. Zhou, Y. Zhang, Y. Hu, L. Lin, Z. L. Wang, "Pyroelectric nanogenerators for harvesting thermoelectric energy" Nano Letters. vol. 12, pp. 2833-2838, April 2012.

[67] G. Zhu, Z. Lin, Q. Jing, P. Bai, C. Pan, Y. Yang, Y. Zhou, and Z. L. Wang "Toward large-scale energy harvesting by a nanoparticle-enhanced triboelectric nanogenerator" Nano Letters vol. 13, pp. 847-853, January 2013.

[68] S. N. Cha, J. Seo, S. Kim, Y. Park, S. Kim and J. Kim, "Sound-driven piezoelectric nanowire-Based nanogenerators" Advanced materials, vol. 22, pp. 4726-4730, August 2010.

[69] F. Fan, Z. Tian and Z. L. Wang, "Flexible triboelectric generator" Nano Energy, vol. 1, pp. 328-334, January 2012.

[70] S. Wang, L. Lin, and Z. L. Wang "Nanoscale triboelectric-effect-enabled energy conversion for sustainably powering portable electronics" Nano Letters, vol. 12, pp. 6339-6346, November 2012.

[71] S. Wang, L. Lin, Y. Xie, Q. Jing, S. Niu, Z. L. Wang, "Sliding-triboelectric nanogenerators based on in-plane charge-separation mechanism", Nano Letters, vol. 13, pp. 2226-2233, April 2013.

[72] Y. Yang, Y. S. Zhou,, H. Zhang, Y. Liu, S. Lee, Z. L. Wang, "A Single-electrode based triboelectric nanogenerator as self-powered tracking system" Advanced Materials, vol. 25, pp. 6594- 6601, October 2013.

[73] Y. Xie, S. Wang, S. Niu, L. Lin, Q. Jing, Y. Su, Z. Wu, Z. L. Wang, "Multi-layered disk triboelectric nanogenerator for Harvesting Hydropower", Nano Energy, vol. 6, pp. 129-136, April 2014.

[74] W. Yang, J. Chen, G. Zhu,, J. Yang, P. Bai, Y. Su, Q. Jing, X. Cao, Z. L. Wang, "Harvesting energy from the natural vibration of human walking" ACS Nano, vol. 7, pp. 11317- 11324, November 2013.

[75] J. Chen, G. Zhu, W. Yang, Q. Jing, P. Bai, Y. Yang, TC. Hou, Z. L. Wang, "Harmonic-resonator-based triboelectric nanogenerator as a sustainable power source and a self-powered active vibration sensor", Advanced Materials, vol. 25, pp. 6094- 6099, 2013, 25, September 2013.

[76] FR. Fan, L. Lin, G. Zhu, W. Wu, R. Zhang, Z. L. Wang, "Transparent triboelectric nanogenerators and self-powered pressure sensors based on micropatterned plastic films", Nano Letters, vol. 12, pp. 3109-3114, May 2012.

[77] G. Zhu, CF. Pan, WX. Guo, CY. Chen, YS. Zhou, RM. Yu, Z. L. Wang, "Triboelectric-generator-driven pulse electrodeposition for micropatterning", Nano Letters, vol. 12, pp. 4960-4965, August 2012.

[78] S. Lee, Y. Lee, D. Kim, Y. Yang, L. Lin, Z.-H. Lin, W. Hwang, Wang, Z. L. Wang, "Triboelectric nanogenerator for harvesting pendulum oscillation energy", Nano Energy, vol. 2, pp. 1113- 1120, September 2013.

[79] Q. Jing, G. Zhu, W. Wu, P. Bai, Y. Xie, R. P. S. Han, Wang, Z. L. Wang, "Self-powered triboelectric velocity sensor for dual-mode sensing of rectified linear and rotary motions", Nano Energy, vol. 10, pp. 305-312, October 2014.

[80] H. Zhang, Y. Yang, Y. Su, J. Chen, K. Adams, S. Lee, C. Hu, Z. L. Wang, "Triboelectric nanogenerator for harvesting vibration energy in full space and as self-powered acceleration sensor. Advanced Functional Materials. vol. 24, pp. 1401- 1407, October 2013.

[81] T. Zho, C. Zhang, C. B. Han, F. R. Fan, W. Tang, Z. L. Wang, "Woven Structured Triboelectric Nanogenerator for Wearable Devices" ACS Applied Materials and Interfaces, vol. 6, pp. 14695-14701, July 2014.

[82] X. Pu, L. Li, H. Song, C. Du, Z. Zhao, C. Jiang, G. Cao, W. Hu, Z. L. Wang, "A Self-Charging Power Unit by Integration of a Textile Triboelectric Nanogenerator and a Flexible Lithium-Ion Battery for Wearable Electronics" Advanced Materials, vol. 27, pp. 2472-2478, March 2015.

[83] Y. H. Ko, G. Nagaraju and J. S. Yu, "Multi-stacked PDMS-based triboelectric generators with conductive textile for efficient energy harvesting", RSC Advances, vol. 5 pp. 6437-6442, December 2014.

[84] S. Lee, W. Ko, Y. Oh, J. Lee, G. Baek, Y. Lee, J. Sohn, S. Cha, J. Kim, J. Park and J. Hong, "Triboelectric energy harvester based on wearable textile platforms employing various surface morphologies", Nano Energy, vol. 12, pp. 410-418, January 2015.

[85] S. Jung, J. Lee, T. Hyeon, M. Lee, DH. Kim, "Fabric-based integrated energy devices for wearable activity monitors", Advanced Materials, vol. 26, pp. 6329-6334, July 2014.

[86] T. Huang, C. Wang, H. Yu, H. Wang, Q. Zhang, M. Zhu, "Human Walking-Driven Wearable All-Fiber Triboelectric Nanogenerator Containing Electrospun Polyvinylidene Fluoride Piezoelectric Nanofibers", Nano Energy vol. 14, pp. 226-235, May 2015.

[87] Z. L. Wang, "Triboelectric Nanogenerators as New Energy Technology for Self-Powered Systems and as Active Mechanical and Chemical Sensors", ACS Nano, vol. 7, pp. 9533-9557, September 2013.

[88] Z. L. Wang, "Triboelectric nanogenerators as new energy technology for self-powered systems and as active mechanical and chemical sensors", ACS Nano, vol. 7, 99. 9533-9557, September 2013.

[89] M. Ma, L. Guo and D. G. Anderson, R. Langer, "Bio-inspired polymer composite actuator and generator driven by water gradients", Science, vol. 339, pp. 186-189, January 2013.

[90] Z. Lin, G. Cheng, L. Lin, S. Lee and Z. L. Wang, "Water-solid surface contact electrification and its use for harvesting liquid wave energy", Angewandte Chemie, vol. 125, pp. 1-6, November 2013.

[91] Q. Liang, X. Yan, Y. Gu, K. Zhang, M. Liang, S. Lu, X. Zheng and Y. Zhang, “Highly transparent triboelectric nanogenerator for harvesting water-related energy reinforced by antireflection coating", Scientific Reports, vol. 13, pp. 1-7, March 2015.

[92] Q. Liang, X. Yan, Y. Gu, K. Zhang, M. Liang, S. Lu, X. Zheng and Y. Zhang, “Highly transparent triboelectric nanogenerator for harvesting water-related energy reinforced by antireflection coating", Sci. Rep., vol. 13, pp. 1-7, March 2015.

[93] Q. Liang, X. Yan, Y. Gu, K. Zhang, M. Liang, S. Lu, X. Zheng and Y. Zhang, “Highly transparent triboelectric nanogenerator for harvesting water-related energy reinforced by antireflection coating", Sci. Rep., vol. 13, pp. 1-7, March 2015.

[94] Q. Liang, X. Yan, Y. Gu, K. Zhang, M. Liang, S. Lu, X. Zheng and Y. Zhang, “Highly transparent triboelectric nanogenerator for harvesting

water-related energy reinforced by antireflection coating", Scientific Reports, vol. 13, pp. 1-7, March 2015.

[95] J. Zhong, Q. Zhong, F. Fan, Y. Zhang, S. Wang, B. Hu, Z. L. Wang and J. Zhou, "Finger typing driven triboelectric nanogenerator and its use for instantaneously lighting up LEDs", Nano Energy, vol. 2, pp. 491-497, July 2013.

[96] W. Seung, M. K. Gupta, K. Y. Lee, K. Shin, J. Lee, T. Y. Kim, S. Kim, J. Lin, J. H. Kim and S. Kim, "Nanopatterned textile-based wearable triboelectric nanogenerator", ACS Nano, vol. 9, pp. 3501-3509, February 2015.

[97] Y. K. Pang, X. H. Li, M. X. Chen, C. B. Han, C. Zhang, and Z. L. Wang, “Triboelectric nanogenerators as a self-powered 3D acceleration sensor", ACS Applied Materials & Interfaces, vol. 7, pp. 19076-19082, August, 2015.

[98] Q. Jing, Y. Xie, G. Zhu, R. P. S. Han and Z. L. Wang, "Self-powered thin-film motion vector sensor", Nature Communications, vol. 6, pp. 1-8, August 2015.

[99] G. Zhu, W. Q Yang, T. Zhang, Q. Jing. J. Chen, Z. L. Wang, "Self-powered ultrasensitive, flexible tactile sensors based on contact electrification", Nano Letters, vol. 14, pp. 3208-3213, May 2014.

[100] P. Bai, G. Zhu, Q. Jing, J. Yang, J. Chen, Y. Su, J. Ma, G. Zhang and Z. L. Wang, "Membrane-based self-powered triboelectric sensors for pressure change detection and its uses in security surveillance and healthcare monitoring", Advanced Functional Materials, vol. 24, pp. 5807-5813 August 2014.

List of Publications

Paper

1) Chang Jun Lee, A Young Choi, Jiwon Park, Hyeon Jun Sim, Changsoon Choi, Seon Jeong Kim and Youn Tae Kim, Triboelectric generator for wearable devices fabricated using casting method, *RSC Advances*, 6, 10094-10098 (2016)

2) A Young Choi, Hyeon Jun Sim, Min Kyoon Shin, Seon Jeong Kim and Youn Tae Kim, Residual charges during electrospinning assist in formation of piezoelectricity in poly(vinylidene fluoride-co-trifluoroethylene) nanofibers, *Journal of Nano Research*, 37, 13-19 (2015)

3) Changsoon Choi, Shi Hyeong Kim, Hyeon Jun Sim, Jae Ah Lee, A Young Choi, Youn Tae Kim, Xavier Lepró, Geoffrey M. Sponks, Ray H. Baughman and Seon Jeong Kim, Stretchable, weavable coiled carbon nanotube/MnO2/polymer fiber solid-state supercapacitors, *Scientific Reports*, 5, 1-6 (2015)

4) Changsoon Choi, Jae Ah Lee, A Young Choi, Youn Tae Kim, Xavier LeprÓ, Marcio D. Lima, Ray H. Baughman and Seon Jeong Kim, Flexible supercapacitor made of carbon nanotube yarn with internal pores, *Advanced Materials*, 26, 2059-2065 (2014)

5) Shi Hyeong Kim, Hyeon Jun Sim, Min Kyoon Shin, A Young Choi, Youn Tae Kim, Marcioo D. Lima, Ray H. Baughman and Seon Jeong Kim, Conductive functional biscrolled polymer and carbon nanotube yarns, *RSC Advances*, 46, 24028-24033 (2013)

List of Publications

Conference

1) "Triboelectric generator made with corrugated stretchable textile for energy harvesting ", Y. S. Kim, J. W. Park, A Y. Choi and Y. T. Kim, MRS Fall Meeting, November 2015

2) "Effects of additional poling process for the electrospun based PVDF-TrFE nanofibers on metal electrode", C. J. Lee, A Y. Choi, H. J. Sim, S. H. Kim, and Y. T. Kim, European Materials Research Society Fall Meeting, September 2013

3) "Piezoelectric ceramic/polymer nanofibers mat for mechanical energy harvesters", C. J. Lee, A Y. Choi, H. J. Sim, S. H. Kim, and Y. T. Kim, European Materials Research Society Fall Meeting, September 2013

4) "Enhanced β Phase Content and Piezoelectric Properties of Electrospun PVDF Nanofibers", A Y. Choi, C. J. Lee, H. J. Sim, M. K. Shin, S. H. Kim, S. J. Kim and Y. T. Kim, Materials Research Society Fall Meeting, November 2012

5) "Conductive Biscrolled Yarn Composite Using Carbon Nanotube Sheets", A Y. Choi, H. J. Sim, M. K. Shin, S. H. Kim, S. J. Kim, M. D. Lima, R. H. Baughman and Y. T. Kim, Materials Research Society Fall Meeting, November 2012

6) "Piezoelectric Polymer Nanofiber Bundle for Mechanical Energy Harvesters", M. K. Shin, S. H. Kim, A Y. Choi, J. A. Lee, H. U. Cho, Y. T. Kim and S. J. Kim, Materials Research Society Spring Meeting, April 2012

7) "Design and Simulation of Energy Harvesting System Based on the CNT/PVDF Nanowired Dielectric Elastomer", A Y. Choi and Y. T. Kim, Materials Research Society Fall Meeting, November 2011

List of Publications

Patent

1) Youn Tae Kim, A Young Choi, Chang Jun Lee, Jiwon Park, Dogyun Kim, "Corrugated textile based triboelectric generator", KR Application Number: 10-2016-0143542

2) Youn Tae Kim, Chang Jun Lee, A Young Choi, Jiwon Park, Dogyun Kim, "Wearable energy generating apparatus", US Application Number: 15/368,807, KR Application Number: 10-2016-00051302

ABSTRACT

Nanostructured Piezoelectric and Textile based Triboelectric Generator for Wearable Energy Harvesting System

A Young Choi
Advisor: Prof. Youn Tae Kim, Ph.D.
Department of IT Fusion Technology,
Graduate School of Chosun University

The main purpose of this study was to develop an wearable energy harvester based on human activities. Wearable energy harvester need to consider parameters such as flexibility, stretchability and comfortability. This study suggest that the piezoelectric response increased as improved polarization by local electric field generated by residual charges, implying that the energy conversion efficiency of the electrospun fibers can be controlled by electrospinning conditions. This study presents the mechanism underlying the additionalpolingofelectrospun fibers by local electric fields originating from residual charges in the far-field electrospinning process. The strength of the local electric field calculated through simulations exceeds the reported strength of near-field electrospinning (10 MV/m). The piezoelectric output of electrospun poly(vinylidene fluoride-co-trifluoroethylene) mats is determined through a push test, and bottom and top output signals are compared. Here the results are consistent with simulation results. This indicates that the piezoelectric output of electrospun fibers can be enhanced by residual charges near the electrode.Triboelecric energy harvesting has been applied to various fields, from large-scale power generation to small electronics.

Triboelectric energy is generated when certain materials come into frictional contact, e.g., static electricity from rubbing a shoe on a carpet. In particular, textile-based triboelectric energy-harvesting technologies are one of the most promising approaches because they are not only flexible, light, and comfortable but also wearable. Most previous textile-based triboelectric generators (TEGs) generate energy by vertically pressing and rubbing something. However, we propose a corrugated textile-based triboelectric generator (CT-TEG) that can generate energy by stretching. Moreover, the CT-TEG is sewn into a corrugated structure that contains an effective air gap without additional spacers. The resulting CT-TEG can generate considerable energy from various deformations, not only by pressing and rubbing but also by stretching. The maximum output voltage of the TEG can reach up to 30.3 V with stretching and releasing motions. Additionally, we demonstrate the generation of sufficient energy from various activities of a human body to power about 55 LEDs. These results demonstrate the potential application of CT-TEGs for self-powered systems.